UV physics from IR features: New prospects from top flavor violation

Wolfgang Altmannshofer[1,*], Stefania Gori[1,†], Benjamin V. Lehmann[2,‡] and Jianhong Zuo[1,§]

[1]*Santa Cruz Institute for Particle Physics and Department of Physics, University of California, Santa Cruz, California 95064, USA*
[2]*Center for Theoretical Physics, Massachusetts Institute of Technology, Cambridge, Massachusetts 02139, USA*

New physics in the rare top decays $t \to q\ell^+\ell^-$ is currently very weakly constrained. We show that in a large class of Standard Model extensions, existing experimental constraints on new physics in flavor-conserving processes imply strong indirect bounds on new physics contributions to flavor-violating processes of the form $t \to q\ell^+\ell^-$. These indirect bounds arise from basic principles of quantum field theory together with a few generic conditions on the UV structure of the theory, and are roughly an order of magnitude stronger than the present experimental bounds on the same processes. These constraints provide a theoretically motivated target for experimental searches for $t \to q\ell^+\ell^-$: violation of these bounds would exclude a large class of new physics models, and would provide nontrivial insight into the UV behavior of the new physics.

I. INTRODUCTION

Flavor-changing neutral current processes involving the top quark are strongly suppressed in the Standard Model (SM) by a loop factor, by small Cabibbo-Kobayashi-Maskawa (CKM) matrix elements, and by an effective Glashow–Iliopoulos–Maiani cancellation. Moreover, these rare top decays compete with the unsuppressed 2-body decay mode $t \to bW$, resulting in extremely small branching ratios to final states like $q\gamma$, qZ, and qh, in the ballpark of 10^{-15} to 10^{-12} for $q = c$ and 10^{-14} to 10^{-17} for $q = u$ [1,2]. The SM predictions for the branching ratios of rare three-body decays of the form $t \to q\ell^+\ell^-$ are smaller yet by approximately two orders of magnitude. Such tiny branching ratios are far below foreseeable experimental sensitivities. The observation of rare top decays at current or planned colliders would therefore be an unambiguous sign of new physics.

Such new physics contributions can typically be accommodated in a single effective field theory (EFT) in which the SM Lagrangian comprises the renormalizable part. The null results in the searches for new physics particles at the LHC may suggest that there is a significant mass gap between the electroweak scale and the new physics scale, meaning that new physics effects can be parametrized by set higher-dimensional operators in a model-independent fashion. This basis of operators, known as the Standard Model EFT (SMEFT) [3], has become a very popular framework to discuss physics beyond the SM (BSM). Existing constraints on rare top decays and other top flavor-violating processes have already been translated to constraints on the Wilson coefficients of SMEFT operators [4–9]. Similarly, measurements of top quark properties, and electroweak precision measurements in general, can be used to constrain the Wilson coefficients of flavor-conserving operators involving top quarks [10–27].

Formulating the new physics contributions in a single EFT presents an opportunity to invoke generic constraints on the form of the SMEFT itself. It has long been known that the possible values of Wilson coefficients in an EFT are restricted not only by experimental results, but also by basic principles of quantum field theory, including unitarity, locality, and analyticity [28]. In the bottom-up approach to constructing an EFT, one typically considers all operators that respect the relevant symmetries and treats the corresponding Wilson coefficients as free parameters that are naively allowed to take arbitrary values. However, not all such low energy scenarios have UV completions. Infrared consistency constraints imply, for example, that certain operators need to have positive Wilson coefficients.

Such constraints have been studied in several cases that are relevant for collider physics, as in the context of

anomalous triple and quartic gauge boson couplings and vector boson scattering at the LHC and future colliders [29–37], fermion–antifermion scattering to dibosons [38,39], or dilepton production [40,41]. It has also been realized that positivity bounds can have implications for flavor-changing operators [42–44]. The results of Ref. [44] are of particular interest in context of rare top decays. Under a small set of assumptions, the Wilson coefficients of certain flavor-violating dimension-six four-fermion operators are bounded by combinations of the Wilson coefficients of flavor-conserving operators.

In many cases, flavor-violating operators lead to very prominent signatures that can be searched for with high precision. Thus, indirect constraints on flavor-violating Wilson coefficients obtained from measurements of flavor-conserving processes are typically subdominant to direct experimental constraints from searches for flavor-violating processes. Rare top decays are a notable exception to this rule. As we show in this paper, the theoretical relations obtained in Ref. [44], combined with experimental constraints on new physics in quark flavor conserving processes, imply that the rare leptonic top decays $t \to q\ell^+\ell^-$ are expected to be approximately an order of magnitude below the current experimental sensitivities in a broad class of new physics models. These expectations provide clear experimental targets for future searches for $t \to q\ell^+\ell^-$ at the LHC and future colliders. Experimental observation of $t \to q\ell^+\ell^-$ above the theoretical expectations would imply that the new physics violates some of the assumptions made in Ref. [44]. Such a measurement would exclude a broad class of new physics models and would imply that the UV structure of the new physics falls into one of a few narrow classes that evades the theoretical constraints.

This paper is organized as follows: In Sec. II, we introduce the EFT setup for the rare top decays and specify the four-fermion operators that we consider in our analysis. In Sec. III, we summarize the results from Ref. [44]. We spell out the theoretical restrictions on the Wilson coefficients and the implications if they were found to be violated. In Sec. IV, we discuss the most relevant experimental constraints. We include existing constraints on flavor-violating rare top decays and single top production, as well as constraints on the flavor-conserving operators from dilepton production at the LHC, atomic parity violation, rare B decays, Z decays, and Møller scattering. Section V contains our main numerical results. Based on the constraints from flavor conserving interactions, we derive the maximal rates for rare top decays and compare them with the existing and expected experimental sensitivities. We discuss the implications of these results and conclude in Sec. VI.

II. EFT SETUP

We consider the following set of dimension-six operators that are subject to sum rules derived in Ref. [44] and that are relevant for rare flavor-changing three-body decays of top quarks $t \to u\ell^+\ell^-$ and $t \to c\ell^+\ell^-$:

$$\mathcal{L}_{\text{eff}} = \frac{1}{\Lambda^2} \left(C_{ijkl}^{\text{LL1}} Q_{ijkl}^{\text{LL1}} + C_{ijkl}^{\text{LL2}} Q_{ijkl}^{\text{LL2}} + C_{ijkl}^{\text{RR}} Q_{ijkl}^{\text{RR}} \right.$$
$$\left. + C_{ijkl}^{\text{LR}} Q_{ijkl}^{\text{LR}} + C_{ijkl}^{\text{RL}} Q_{ijkl}^{\text{RL}} \right). \tag{1}$$

The definitions of the various operators are

$$Q_{ijkl}^{\text{LL1}} = (\bar{\ell}_i \gamma_\mu \ell_j)(\bar{q}_k \gamma^\mu q_l), \tag{2}$$

$$Q_{ijkl}^{\text{LL2}} = (\bar{\ell}_i \gamma_\mu \tau^I \ell_j)(\bar{q}_k \gamma^\mu \tau^I q_l), \tag{3}$$

$$Q_{ijkl}^{\text{RR}} = (\bar{e}_i \gamma_\mu e_j)(\bar{u}_k \gamma^\mu u_l), \tag{4}$$

$$Q_{ijkl}^{\text{LR}} = (\bar{\ell}_i \gamma_\mu \ell_j)(\bar{u}_k \gamma^\mu u_l), \tag{5}$$

$$Q_{ijkl}^{\text{RL}} = (\bar{e}_i \gamma^\mu e_j)(\bar{q}_k \gamma_\mu q_l), \tag{6}$$

where τ^I denotes the Pauli matrices for $I = 1, 2, 3$; ℓ_i are the three generations of left-handed lepton doublets; e_i the right-handed charged lepton singlets; q_i are the left-handed quark doublets; and u_i the right-handed quark singlets of up-type. In the effective Lagrangian of Eq. (1), a sum over the flavor indices i, j, k, l is understood. Note that our notation differs from the standard SMEFT notation of Ref. [3] that is often used in the literature. In the above Lagrangian, we do not include additional four-fermion operators with scalar or tensor currents or dipole operators. Such operators can also lead to rare top decays, but they are not subject to the sum rules derived in Ref. [44].

The sum rules are based on analyticity of the S-matrix, partial wave unitarity, and assumptions about the high momentum behavior of forward scattering amplitudes. If the new physics in the UV is dominated by either scalars or vectors, the sum rules imply definite signs of certain combinations of Wilson coefficients. (See also Refs. [45–47].) Defining $C_{\alpha\beta} = \alpha_i \alpha_j^* \beta_k^* \beta_l C_{ijkl}$, where α and β are arbitrary directions in flavor space, the constraints can be summarized in the following way:

$$s \left(C_{\alpha\beta}^{\text{LL1}} \pm \frac{1}{4} C_{\alpha\beta}^{\text{LL2}} \right) > 0,$$
$$s C_{\alpha\beta}^{\text{RR}} > 0, \qquad s C_{\alpha\beta}^{\text{LR}} < 0, \quad \text{and} \quad s C_{\alpha\beta}^{\text{RL}} < 0, \tag{7}$$

where $s = +1 \ (-1)$ if the UV contributions to the Wilson coefficients are dominated by scalars (vectors). If both scalars and vectors contribute at a comparable level to the Wilson coefficients, cancellations may occur, so the sign of s cannot be established from first principles.

Many operators that lead to rare top decays are strongly constrained by flavor-changing neutral current processes involving B mesons [48]. In particular, in the presence of

the operators in Eq. (1) that contain left-handed quark fields, $SU(2)_L$ gauge invariance implies that sizable rates of $t \to c(u)\ell^+\ell^-$ decays are directly related to large new physics effects in $b \to s(d)\ell^+\ell^-$ or $b \to s(d)\nu\bar{\nu}$ decays. Barring tuned cancellations, the strong experimental constraints on the rare B decays exclude rare top decays at an experimentally accessible level. As we will discuss in Sec. IV C 1, for operators that contain right-handed up-type quarks, constraints from rare B decays only arise at the loop level, leaving much more room for sizable rare top branching ratios. In the following, we will thus focus on the operators Q^{LR} and Q^{RR}. Furthermore, we will only consider operators with electrons or muons. Operators with taus could be included in an analogous way, but are much more challenging to probe experimentally. The interactions that we are interested in can be split into lepton-flavor–conserving and lepton-flavor–violating operators. The ones that conserve lepton flavor are explicitly given by

$$
\begin{aligned}
\Lambda^2 \mathcal{L}_{\text{eff}}^{\text{LFC}} =\ & C_{eett}^{\text{LR}}[(\bar{\nu}_e\gamma_\alpha P_L\nu_e) + (\bar{e}\gamma_\alpha P_L e)](\bar{t}\gamma^\alpha P_R t) + C_{eett}^{\text{RR}}(\bar{e}\gamma_\alpha P_R e)(\bar{t}\gamma^\alpha P_R t) \\
& + C_{eecc}^{\text{LR}}[(\bar{\nu}_e\gamma_\alpha P_L\nu_e) + (\bar{e}\gamma_\alpha P_L e)](\bar{c}\gamma^\alpha P_R c) + C_{eecc}^{\text{RR}}(\bar{e}\gamma_\alpha P_R e)(\bar{c}\gamma^\alpha P_R c) \\
& + \left(C_{eect}^{\text{LR}}[(\bar{\nu}_e\gamma_\alpha P_L\nu_e) + (\bar{e}\gamma_\alpha P_L e)](\bar{c}\gamma^\alpha P_R t) + C_{eect}^{\text{RR}}(\bar{e}\gamma_\alpha P_R e)(\bar{c}\gamma^\alpha P_R t) + \text{H.c.} \right) + \cdots,
\end{aligned} \tag{8}
$$

where the ellipsis corresponds to terms where electrons and electron neutrinos are replaced with muons and muon neutrinos, or charm quarks are replaced with up quarks, as appropriate. The lepton-flavor-violating terms are given by

$$
\begin{aligned}
\Lambda^2 \mathcal{L}_{\text{eff}}^{\text{LFV}} =\ & \left(C_{e\mu tt}^{\text{LR}}[(\bar{\nu}_e\gamma_\alpha P_L\nu_\mu) + (\bar{e}\gamma_\alpha P_L\mu)](\bar{t}\gamma^\alpha P_R t) + C_{e\mu tt}^{\text{RR}}(\bar{e}\gamma_\alpha P_R\mu)(\bar{t}\gamma^\alpha P_R t) + \text{H.c.} \right) \\
& + \left(C_{e\mu cc}^{\text{LR}}[(\bar{\nu}_e\gamma_\alpha P_L\nu_\mu) + (\bar{e}\gamma_\alpha P_L\mu)](\bar{c}\gamma^\alpha P_R c) + C_{e\mu cc}^{\text{RR}}(\bar{e}\gamma_\alpha P_R\mu)(\bar{c}\gamma^\alpha P_R c) + \text{H.c.} \right) \\
& + \left(C_{e\mu ct}^{\text{LR}}[(\bar{\nu}_e\gamma_\alpha P_L\nu_\mu) + (\bar{e}\gamma_\alpha P_L\mu)](\bar{c}\gamma^\alpha P_R t) + C_{e\mu ct}^{\text{RR}}(\bar{e}\gamma_\alpha P_R\mu)(\bar{c}\gamma^\alpha P_R t) \right. \\
& \left. + C_{\mu ect}^{\text{LR}}[(\bar{\nu}_\mu\gamma_\alpha P_L\nu_e) + (\bar{\mu}\gamma_\alpha P_L e)](\bar{c}\gamma^\alpha P_R t) + C_{\mu ect}^{\text{RR}}(\bar{\mu}\gamma_\alpha P_R e)(\bar{c}\gamma^\alpha P_R t) + \text{H.c.} \right) + \cdots,
\end{aligned} \tag{9}
$$

with the ellipsis indicating terms in which charm quarks are replaced with up quarks.

III. THEORETICAL CONSTRAINTS ON THE WILSON COEFFICIENTS

If the relations in Eq. (7) hold, one can derive constraints on the flavor-specific Wilson coefficients in Eqs. (8) and (9). In particular, the flavor conserving Wilson coefficients have definite signs: if the UV is dominated by scalars, then

$$
C_{\ell\ell qq}^{\text{LR}} < 0 \quad \text{and} \quad C_{\ell\ell qq}^{\text{RR}} > 0, \tag{10}
$$

while if the UV is dominated by vectors, then

$$
C_{\ell\ell qq}^{\text{LR}} > 0 \quad \text{and} \quad C_{\ell\ell qq}^{\text{RR}} < 0. \tag{11}
$$

In either case, one finds that the flavor-violating coefficients are bounded from above by the flavor-conserving ones as [42,44]

$$
\begin{aligned}
|C_{eect}^{\text{LR}}|^2 &< C_{eecc}^{\text{LR}} C_{eett}^{\text{LR}}, & |C_{\mu\mu ct}^{\text{LR}}|^2 &< C_{\mu\mu cc}^{\text{LR}} C_{\mu\mu tt}^{\text{LR}}, \\
|C_{eect}^{\text{RR}}|^2 &< C_{eecc}^{\text{RR}} C_{eett}^{\text{RR}}, & |C_{\mu\mu ct}^{\text{RR}}|^2 &< C_{\mu\mu cc}^{\text{RR}} C_{\mu\mu tt}^{\text{RR}}.
\end{aligned} \tag{12}
$$

If both scalar and vector contributions are comparable, there can be cancellations and no bounds can be established. Analogous bounds hold for lepton-flavor–violating and quark-flavor–conserving interactions. The case of interactions that violate both quark and lepton flavor is nontrivial, and we leave a detailed exploration for future work.

The relations in Eq. (12) have very interesting implications. One can combine existing experimental constraints from flavor conserving processes on nonstandard interactions of $\ell\ell uu$, $\ell\ell cc$, and $\ell\ell tt$ to derive upper bounds on the rare top decays $t \to u\ell^+\ell^-$ and $t \to c\ell^+\ell^-$. These upper bounds then serve as targets for experimental searches. If rare top decays are observed above the bounds, one or more of the hypotheses of the theoretical bounds must be violated. Possible options are

(1) The rare top decays are induced by effective interactions other than the ones spelled out in Eq. (8)—for example, by operators with scalar or tensor currents.

(2) The UV physics that generates the effective interactions is not dominated by either scalars or vectors. For example, both scalars and vectors could contribute at a comparable level such that nontrivial cancellations take place.

(3) The UV physics gives forward-scattering amplitudes that grow with s^n for $n \geq 1$, where s is the squared center-of-mass energy [44,49]. For example, this can happen if the forward scattering is mediated by vectors in the t-channel.

Therefore, the observation of a violation of the theoretical bounds allows one to exclude entire classes of possible UV models that lead to rare top decays.

IV. EXPERIMENTAL CONSTRAINTS ON THE WILSON COEFFICIENTS

In this section, we discuss the most relevant experimental constraints on the Wilson coefficients.

(i) In Sec. IV A, we start with a discussion of processes that are induced by the top-flavor-violating operators in Eqs. (8) and (9). We consider rare flavor-violating top decays at the LHC and single top production at e^+e^- colliders.

(ii) In Sec. IV B, we discuss the most relevant processes that constrain flavor-conserving operators with light quarks. This includes, in particular, high-mass tails in dilepton production at the LHC, as well as parity violation in low-energy electron-proton scattering.

(iii) Finally, in Sec. IV C, we discuss constraints on flavor-conserving operators containing top quarks, including rare B decays, decays of the Z boson, and parity violation in Møller scattering. In principle, LHC measurements of the production cross section for $t\bar{t}$ and single top quarks are sensitive to the flavor conserving four-fermion operators with top quarks. The constraints from the CMS analysis of Ref. [50] are weaker than the ones we find from Z decays and B decays, so we do not consider them here.

In all cases, we derive the expressions for the new physics contributions to the relevant observables, discuss the existing experimental bounds, and comment on the expected future sensitivities. We list constraints on all Wilson coefficients in Table III.

We note that the operators in Eqs. (8) and (9) also contain neutrinos. They can therefore modify the production of neutrinos at the LHC as well as the neutrino–nucleus scattering cross section measured at neutrino experiments. Nonstandard neutrino production at the LHC can be constrained by mono-X searches. The most stringent bounds come from monojet searches Ref. [51,52]. However, we do not consider them in detail in this paper, since they are weaker than the bounds from LHC dilepton spectrum measurements that we discuss in Sec. IV B 1. New physics contributions to neutrino–nucleus scattering are constrained by e.g. the results from the COHERENT experiment [53]. Bounds on the operators with up quarks and neutrinos have been derived in Ref. [54], and these bounds are indeed subdominant to the other bounds we consider.

A. Flavor-violating processes

1. Rare top decays

The effective couplings $C_{\ell\ell tq}^{\mathrm{LR}}$ and $C_{\ell\ell tq}^{\mathrm{RR}}$ enable the rare flavor-changing three-body top decays $t \to q\ell^+\ell^-$, where $q \in \{u, c\}$ and $\ell \in \{e, \mu\}$. Normalizing to the dominant $t \to Wb$ decay mode of the top quark, we find the leading-order branching ratios as

$$\mathrm{BR}(t \to q\ell^+\ell^-) \simeq \frac{1}{96\pi^2}\frac{m_t^2 v^2}{\Lambda^4}(|C_{\ell\ell tq}^{\mathrm{LR}}|^2 + |C_{\ell\ell tq}^{\mathrm{RR}}|^2)$$
$$\times \left(1 - \frac{m_W^2}{m_t^2}\right)^{-2}\left(1 + \frac{2m_W^2}{m_t^2}\right)^{-1}. \quad (13)$$

Lepton flavor changing decays are also possible, with the leading-order branching ratios

$$\mathrm{BR}(t \to q\ell\ell') \simeq \frac{1}{96\pi^2}\frac{m_t^2 v^2}{\Lambda^4}(|C_{\ell\ell' tq}^{\mathrm{LR}}|^2 + |C_{\ell\ell' tq}^{\mathrm{RR}}|^2$$
$$+ |C_{\ell'\ell tq}^{\mathrm{LR}}|^2 + |C_{\ell'\ell tq}^{\mathrm{RR}}|^2)$$
$$\times \left(1 - \frac{m_W^2}{m_t^2}\right)^{-2}\left(1 + \frac{2m_W^2}{m_t^2}\right)^{-1}, \quad (14)$$

where $\mathrm{BR}(t \to q\ell\ell') \equiv \mathrm{BR}(t \to q\ell^+\ell'^-) + \mathrm{BR}(t \to q\ell'^+\ell^-)$. Our expressions for the branching ratios are consistent with the results in Ref. [7].

At the LHC, $t\bar{t}$ pairs are produced copiously, and searches have been conducted for the flavor-violating two-body decays $t \to qH$, $t \to qZ$, and $t \to q\gamma$. However, no direct searches for the three-body decays $t \to q\ell\ell$ exist so far. Bounds have been obtained in Ref. [7] by recasting an ATLAS search for the decays $t \to Zq$ [55] based on ~ 36 fb^{-1} of Run II data, taking into account the full set of dimension-six operators that can lead to the $t \to q\ell\ell$ decays. (See Ref. [56] for a related CMS search.) As we restrict our analysis to the vector operators $Q_{\ell\ell tq}^{\mathrm{RR}}$ and $Q_{\ell\ell tq}^{\mathrm{LR}}$, we can translate the results of Ref. [7] into bounds on the $t \to q\ell^+\ell^-$ branching ratios. We find, at 95% confidence level (CL),

$$\mathrm{BR}(t \to ce^+e^-) < 2.1 \times 10^{-4},$$
$$\mathrm{BR}(t \to ue^+e^-) < 1.8 \times 10^{-4},$$
$$\mathrm{BR}(t \to c\mu^+\mu^-) < 1.5 \times 10^{-4},$$
$$\mathrm{BR}(t \to u\mu^+\mu^-) < 1.2 \times 10^{-4}. \quad (15)$$

This translates into the following (rather weak) bounds on the new physics scale:

$$\frac{|C_{eect}^{\mathrm{LR}}|}{\Lambda^2}, \frac{|C_{eect}^{\mathrm{RR}}|}{\Lambda^2} < \frac{1}{(0.32 \text{ TeV})^2}, \quad (16)$$

$$\frac{|C_{eeut}^{\text{LR}}|}{\Lambda^2}, \frac{|C_{eeut}^{\text{RR}}|}{\Lambda^2} < \frac{1}{(0.33 \text{ TeV})^2}, \tag{17}$$

$$\frac{|C_{\mu\mu ct}^{\text{LR}}|}{\Lambda^2}, \frac{|C_{\mu\mu ct}^{\text{RR}}|}{\Lambda^2} < \frac{1}{(0.35 \text{ TeV})^2}, \tag{18}$$

$$\frac{|C_{\mu\mu ut}^{\text{LR}}|}{\Lambda^2}, \frac{|C_{\mu\mu ut}^{\text{RR}}|}{\Lambda^2} < \frac{1}{(0.36 \text{ TeV})^2}. \tag{19}$$

A dedicated search for $t \to q\ell^+\ell^-$ at the High-Luminosity LHC might improve the above bounds on the branching ratios by almost two orders of magnitude [7], corresponding to an improvement by a factor of ~ 3 in sensitivity to the new physics scale. A future 100 TeV collider might improve the sensitivity to rare top decay rates by another order of magnitude [57]. Improved sensitivity might also be obtained from searches for single top production in association with same-flavor dileptons [9].

LHC searches for rare lepton-flavor–violating top decays $t \to q\mu e$ have been proposed in Ref. [58]. It was estimated that with a center-of-mass energy of $\sqrt{s} = 13$ TeV and an integrated luminosity of 100 fb^{-1}, the LHC could probe the branching ratios BR($t \to q\mu e$) to the level of $\sim 10^{-5}$. The first results from searches for lepton flavor violation in top decays in ~ 80 fb^{-1} of ATLAS data [59] and ~ 137 fb^{-1} of CMS data [60] have not observed any significant excess above expected SM backgrounds, placing bounds on the branching ratios. The CMS analysis of Ref. [60] considers not only $t\bar{t}$ production with a subsequent lepton-flavor–violating decay by one of the top quarks, but also single top production in association with μe. The results from searches for the flavor-changing decays and production are combined assuming the presence of a specific set of contact interactions and recast in terms of a bound on the branching ratio. For vector interactions, as in the case we study here, the bounds at 95% CL are [60,61]

$$\text{BR}(t \to c\mu e) < 1.3 \times 10^{-6},$$
$$\text{BR}(t \to u\mu e) < 1.3 \times 10^{-7}. \tag{20}$$

Considering one lepton-flavor-violating top quark operator at a time, and assuming that the CMS bound on the vector interactions does not depend on the chirality of the quarks and leptons involved in the transition, these bounds correspond to

$$\frac{|C_{\mu etc}^{\text{LR}}|}{\Lambda^2}, \frac{|C_{\mu etc}^{\text{RR}}|}{\Lambda^2}, \frac{|C_{e\mu tc}^{\text{LR}}|}{\Lambda^2}, \frac{|C_{e\mu tc}^{\text{RR}}|}{\Lambda^2} < \frac{1}{(1.1 \text{ TeV})^2},$$
$$\frac{|C_{\mu etu}^{\text{LR}}|}{\Lambda^2}, \frac{|C_{\mu etu}^{\text{RR}}|}{\Lambda^2}, \frac{|C_{e\mu tu}^{\text{LR}}|}{\Lambda^2}, \frac{|C_{e\mu tu}^{\text{RR}}|}{\Lambda^2} < \frac{1}{(2.0 \text{ TeV})^2}. \tag{21}$$

Assuming that sensitivity to the branching ratio scales with the square root of integrated luminosity, we expect improvement by a factor of ~ 5 at the high-luminosity LHC. This corresponds to an improvement by a factor of ~ 1.5 in reach to the new physics scale.

2. Single top production

Single top production in lepton collisions, $\ell^+\ell^- \to tq$, with $q \in \{u, c\}$, has been identified as an important probe of top-flavor–changing contact interactions [5,62–64]. The tree-level production cross section from e^+e^- collisions,

$$\sigma(e^+e^- \to tq) = \sigma(e^+e^- \to t\bar{q}) + \sigma(e^+e^- \to \bar{t}q), \tag{22}$$

can be written in the following way:

$$\sigma(e^+e^- \to tq) = \frac{1}{6\pi} \frac{s}{\Lambda^4} \left(1 - \frac{m_t^2}{s}\right)^2 \left(1 + \frac{m_t^2}{2s}\right)$$
$$\times \left(|C_{eetq}^{\text{LR}}|^2 + |C_{eetq}^{\text{RR}}|^2\right), \tag{23}$$

where s is the squared center-of-mass energy. In our setup, single top production is sensitive to the exact same combination of Wilson coefficients as the $t \to qe^+e^-$ decays.

Single top production has been searched for at LEP [65–67]. We use the combined results from all LEP experiments, reported in Ref. [65]. We find that the strongest constraint on the flavor-changing effective interactions can be obtained from the quoted bound on the cross section at a center-of-mass energy of $\sqrt{s} = 189$ GeV, resulting in the bound

$$\sigma(e^+e^- \to tq) < 0.11 \text{ pb}. \tag{24}$$

We do not attempt to combine this bound with others that are given at different center-of-mass energies. As no flavor-tagging of the light quarks has been performed in Ref. [65], we interpret the bound in Eq. (24) as a bound on the combined cross section $\sigma(e^+e^- \to tq) = \sigma(e^+e^- \to tu) + \sigma(e^+e^- \to tc)$. Switching on one effective operator at a time, and taking into account only the bound on the cross section quoted above, we find the following constraints on the Wilson coefficients:

$$\frac{|C_{eect}^{\text{LR}}|}{\Lambda^2}, \frac{|C_{eect}^{\text{RR}}|}{\Lambda^2}, \frac{|C_{eeut}^{\text{LR}}|}{\Lambda^2}, \frac{|C_{eeut}^{\text{RR}}|}{\Lambda^2} < \frac{1}{(0.7 \text{ TeV})^2}. \tag{25}$$

The bound on the new physics scale is stronger by a factor of ~ 2 compared to the bounds from the rare top decays $t \to qe^+e^-$ discussed in the previous subsection.

Future e^+e^- colliders [68–70] can improve the sensitivity considerably. In Ref. [8], it is estimated that at CEPC, with a center-of-mass energy of $\sqrt{s} = 240$ GeV and an integrated luminosity of 5.6 ab^{-1}, new physics could be probed at a scale of several TeV. Similar sensitivities can be expected at FCC-ee and at the ILC.

At an e^+e^- collider, the muonic operators also affect single top production, albeit only at the loop level. We have calculated the corresponding one-loop contribution to the cross section and found very weak constraints on the new physics scale, on the order of a few $\times 10$ GeV. This lies outside the regime of validity of the EFT, so no actual constraint can be obtained. We expect strong sensitivity to the muonic operators from single top production at a future high-energy muon collider [64,71].

Finally, single top production in ep collisions can also be used to constrain top-flavor–changing contact interactions. The process $ep \to etX$ has been searched for at HERA, and bounds on the corresponding cross sections have been obtained in Refs. [72,73]. These results can be used to constrain the Wilson coefficients C_{eeut}^{LR} and C_{eeut}^{RR}. However, the constraints from $e^+e^- \to tq$ at LEP turn out to be stronger [5,8]. We therefore do not consider single top production at ep colliders for the remainder of this work.

B. Light quark flavor-conserving processes

1. Dilepton spectra at the LHC

Measurements of the dilepton invariant mass distribution at the LHC are well established as probes of new physics in the form of quark-lepton contact interactions [74–79]. In the SM, for sufficiently large partonic center-of-mass energy $\sqrt{\hat{s}}$, the Drell-Yan parton-level cross sections $\hat{\sigma}_q = \sigma(q\bar{q} \to \ell^+\ell^-)$ fall with $\hat{s}$, but they grow with $\hat{s}$ in the presence of the contact interactions. We find

$$\hat{\sigma}_q(\hat{s}) = \frac{\hat{s}}{144\pi} \sum_{\mathrm{X,Y}\in\{\mathrm{L,R}\}} |A_q^{\mathrm{XY}}|^2, \tag{26}$$

where in the limit $\hat{s} \gg m_Z^2$, the amplitudes can be approximated at leading order by

$$-iA_q^{\mathrm{LL}} = \frac{1}{\hat{s}} e^2 Q_\ell Q_q + \frac{1}{\hat{s}} \frac{e^2}{s_W^2 c_W^2} Q_{\ell_L}^{\mathrm{w}} Q_{q_L}^{\mathrm{w}}, \tag{27}$$

$$-iA_q^{\mathrm{LR}} = \frac{1}{\hat{s}} e^2 Q_\ell Q_q + \frac{1}{\hat{s}} \frac{e^2}{s_W^2 c_W^2} Q_{\ell_L}^{\mathrm{w}} Q_{q_R}^{\mathrm{w}} + \frac{1}{\Lambda^2} C_{\ell\ell qq}^{\mathrm{LR}}, \tag{28}$$

$$-iA_q^{\mathrm{RL}} = \frac{1}{\hat{s}} e^2 Q_\ell Q_q + \frac{1}{\hat{s}} \frac{e^2}{s_W^2 c_W^2} Q_{\ell_R}^{\mathrm{w}} Q_{q_L}^{\mathrm{w}}, \tag{29}$$

$$-iA_q^{\mathrm{RR}} = \frac{1}{\hat{s}} e^2 Q_\ell Q_q + \frac{1}{\hat{s}} \frac{e^2}{s_W^2 c_W^2} Q_{\ell_R}^{\mathrm{w}} Q_{q_R}^{\mathrm{w}} + \frac{1}{\Lambda^2} C_{\ell\ell qq}^{\mathrm{RR}}. \tag{30}$$

Here Q_f denotes the electric charges of the leptons and quarks, and $Q_f^{\mathrm{w}} = T_3^f - s_W^2 Q_f$ denotes their weak charges. In the absence of the new-physics contact interactions, $-iA_q^{\mathrm{LR}}$ and $-iA_q^{\mathrm{RR}}$ are negative for up-type quarks. If the new physics effect is mediated by scalars, the theoretical

bounds on the Wilson coefficients $C_{\ell\ell qq}^{\mathrm{LR}}$ and $C_{\ell\ell qq}^{\mathrm{RR}}$ from Eq. (10) predict constructive interference in $A_{u,c}^{\mathrm{LR}}$ and destructive interference in $A_{u,c}^{\mathrm{RR}}$. Conversely, if the new physics effect is mediated by vectors, Eq. (11) implies destructive interference in $A_{u,c}^{\mathrm{LR}}$ and constructive interference in $A_{u,c}^{\mathrm{RR}}$.

Due to the growth with $\hat{s}$, the high invariant mass tails in $pp \to \ell^+\ell^-$ are very sensitive to new-physics contact interactions. Consider a proton–proton scattering process with center-of-mass energy $\sqrt{s}$. The integrated cross section at large dilepton invariant mass $m_{\ell\ell}$ is given by

$$\sigma(pp \to \ell^+\ell^-) = \sum_q \int_{\tau_{\min}}^{\tau_{\max}} \mathrm{d}\tau \, 2\mathcal{L}_{q\bar{q}}(\tau)\hat{\sigma}_q(s\tau), \tag{31}$$

where $\tau = m_{\ell\ell}^2/s$, with the parton luminosities given by

$$\mathcal{L}_{q\bar{q}}(\tau) = \int_\tau^1 \frac{\mathrm{d}x}{x} f_q(x) f_{\bar{q}}(\tau/x). \tag{32}$$

For our numerical analysis we include $q \in \{u, d, s, c\}$, and use the parton distribution functions f_q and $f_{\bar{q}}$ from Ref. [80], setting the factorization scale to the dynamical value $\mu_{\mathrm{F}} = m_{\ell\ell}$.

We use the ATLAS analysis of Ref. [75] to constrain the Wilson coefficients $C_{\ell\ell qq}^{\mathrm{LR}}$ and $C_{\ell\ell qq}^{\mathrm{RR}}$, for $\ell \in \{e, \mu\}$ and $q \in \{u, c\}$. Similar constraints could be obtained from an analogous CMS analysis [76]. At high $m_{\ell\ell}$, the main dilepton background to the new-physics signal is from SM Drell-Yan production, with only percent-level contributions from other background sources like $t\bar{t}$, single top, dibosons, or misidentified jets [75,76]. Using Madgraph5_aMC@NLO [81], we explicitly checked that the product of acceptance and efficiency is very similar for SM Drell–Yan events and signal events in the presence of the contact interactions. We thus approximate the number of signal events N_{sig}^ℓ in a given signal region as

$$N_{\mathrm{sig}}^\ell = N_{\mathrm{bg}}^\ell \left(\frac{\sigma(pp \to \ell^+\ell^-)}{\sigma(pp \to \ell^+\ell^-)_{\mathrm{SM}}} - 1 \right), \tag{33}$$

where N_{bg}^ℓ is the number of expected background events.

The ATLAS analysis uses signal regions that are optimized for either destructive or constructive interference. In our scenarios both destructive and constructive interference can occur, and in each case we use the signal regions that result in the stronger constraint. The signal regions optimized for constructive (destructive) interference are defined by $\tau_{\min} = 2.2$ TeV (2.77 TeV) for electrons and $\tau_{\min} = 2.07$ TeV (2.57 TeV) for muons. In all cases, $\tau_{\max} = 6.0$ TeV. The corresponding numbers of expected SM background events are $N_{\mathrm{bg}}^e = 12.4$ (3.1) and $N_{\mathrm{bg}}^\mu = 9.6$ (1.4) for electrons and for muons, respectively.

TABLE I. Bounds on the EFT scale in TeV units extracted from the LHC dilepton spectrum, measured in Ref. [75]. Each row corresponds to a bound of the form $-1/\Lambda_-^2 < C/\Lambda^2 < 1/\Lambda_+^2$, with all other coefficients set to zero.

Coefficient	Λ_-	Λ_+	Coefficient	Λ_-	Λ_+
C_{eeuu}^{LR}	8.0	6.5	$C_{\mu\mu uu}^{\mathrm{LR}}$	8.0	5.9
C_{eeuu}^{RR}	8.8	5.9	$C_{\mu\mu uu}^{\mathrm{RR}}$	9.2	5.1
C_{eecc}^{LR}	2.0	2.0	$C_{\mu\mu cc}^{\mathrm{LR}}$	2.1	2.0
C_{eecc}^{RR}	2.0	2.0	$C_{\mu\mu cc}^{\mathrm{RR}}$	2.1	2.0

To obtain the bounds on the Wilson coefficients, we impose the model-independent upper limits at 95% CL on the number of signal events: $N_{\mathrm{sig}}^{e} < 16.0$ (4.4) for electrons, and $N_{\mathrm{sig}}^{\mu} < 5.8$ (3.8) for muons [75], in the signal regions optimized for constructive (destructive) interference. We have checked that this procedure reproduces the given bounds on the contact interactions studied in Ref. [75], finding agreement within 15%.

Switching on one operator at a time, we find the constraints in Table I. As expected, the strongest constraints are obtained for operators containing up quarks. We can estimate that at the high-luminosity LHC, which will increase the total luminosity by a factor of $\sim$20, the constraints on σ will be improved by a factor of $\sim$4, and those on Λ can therefore be improved by a factor of $\sim$2. This scaling represents only a rough estimate of the reach of the HL-LHC. A dedicated study along the lines of Ref. [82] would be needed to assess the exact bound.

The electron-quark contact interactions can also be constrained from dijet production at LEP. The constraints on electron-charm interactions reported in Ref. [83] are comparable to the ones given above. In the case of electron-up interactions, the LHC constraints are considerably stronger.

Note that high-mass dilepton tails at the LHC can also be used to constrain lepton-flavor–violating and quark-flavor–conserving four-fermion contact interactions [84]. However, the theoretical relations among the Wilson coefficients that we consider in this work [Eq. (12)] do not involve such contact interactions, so we will not consider these constraints.

2. Atomic parity violation and electron nucleus scattering

Experiments measuring atomic parity violation are sensitive probes of new physics at the TeV scale [85]. The most constraining result is currently a precision measurement of a parity-violating electric dipole transition in Cesium [86,87]. Atomic parity violation is induced by the SM weak interaction, but can receive contributions from parity-violating new physics as well. The Cesium measurement can be interpreted in terms of the nuclear weak charge, Q_W, which receives new physics contributions from the flavor-conserving operators in Eq. (8) that contain up quarks and electrons. The correction to Q_W is given by

$$\frac{\delta Q_W}{Q_W^{\mathrm{SM}}} = \frac{v^2}{\Lambda^2}(C_{eeuu}^{\mathrm{RR}} - C_{eeuu}^{\mathrm{LR}})\frac{2\mathcal{Z} + \mathcal{N}}{\mathcal{N} - \mathcal{Z}(1 - 4s_W^2)}, \quad (34)$$

where $v = 246$ GeV is the vacuum expectation value (vev) of the Higgs, and $\mathcal{Z}$ and $\mathcal{N}$ are the numbers of protons and neutrons in the nucleus, respectively. Combining the Cesium measurement with the SM prediction for Q_W, one finds $Q_W^{\mathrm{exp}} - Q_W^{\mathrm{SM}} = -0.48 \pm 0.35$ [87], which at 95% CL gives

$$-0.3\% < \frac{\delta Q_W}{Q_W^{\mathrm{SM}}} < 1.6\%. \quad (35)$$

This translates into the following constraints on the Wilson coefficients:

$$-\frac{1}{(7.2 \text{ TeV})^2} < \frac{C_{eeuu}^{\mathrm{RR}}}{\Lambda^2} - \frac{C_{eeuu}^{\mathrm{LR}}}{\Lambda^2} < \frac{1}{(3.1 \text{ TeV})^2}. \quad (36)$$

The constraints from dilepton production at the LHC discussed in the previous section are more stringent (see Table I).

A recent proposal has the potential to improve on this result. The measurements of elastic electron–proton or electron–^{12}C scattering at the proposed P2 experiment [88] at the Mainz Energy-recovering Superconducting Accelerator (MESA) facility can give a more stringent bound on these operators. The basic idea is to measure the parity-violating asymmetry,

$$A_{\mathrm{LR}} = \frac{\sigma_L - \sigma_R}{\sigma_L + \sigma_R}, \quad (37)$$

where σ_L (σ_R) is the cross section for the scattering of electrons with left (right) helicity. The asymmetry is directly related to the nuclear weak charge as

$$\frac{\delta A_{\mathrm{LR}}}{A_{\mathrm{LR}}^{\mathrm{SM}}} = \frac{\delta Q_W}{Q_W^{\mathrm{SM}}}. \quad (38)$$

The relative uncertainties $\delta A_{\mathrm{LR}}/A_{\mathrm{LR}}^{\mathrm{SM}}$ are expected to be 1.4% and 0.3% for electron–proton and electron–^{12}C scattering, respectively [88]. This translates into the 95% CL bounds

$$\left|\frac{C_{eeuu}^{\mathrm{RR}}}{\Lambda^2} - \frac{C_{eeuu}^{\mathrm{LR}}}{\Lambda^2}\right| < \frac{1}{(7.5 \text{ TeV})^2} \quad (e^- - p^+)$$

$$\left|\frac{C_{eeuu}^{\mathrm{RR}}}{\Lambda^2} - \frac{C_{eeuu}^{\mathrm{LR}}}{\Lambda^2}\right| < \frac{1}{(5.7 \text{ TeV})^2} \quad (e^- - {}^{12}\text{C}). \quad (39)$$

These results are similar to those in Refs. [89,90]. For the numerical evaluation, we use $s_W^2 = 0.231$, corresponding to

the $\overline{\text{MS}}$ value at the Z-pole. For the scattering with protons, one can expect sizable higher-order corrections due to the accidental suppression of the SM asymmetry $A_{\text{LR}}^{\text{SM}} \propto 1-4s_W^2$. The resulting projected bounds are comparable to the current LHC bounds shown in Table I.

C. Heavy quark flavor conserving processes

1. Rare B decays

Rare decays of b hadrons based on the $b \to see$ and $b \to s\mu\mu$ transitions are sensitive probes of new physics [91,92] and can be used to constrain both the flavor-conserving and the flavor-changing top quark operators. New physics contributions to rare B decays are usually phrased in terms of an effective Hamiltonian

$$\mathcal{H}_{\text{eff}} = \mathcal{H}_{\text{eff}}^{\text{SM}} - \frac{4G_F}{\sqrt{2}} V_{tb}V_{ts}^* \frac{e^2}{16\pi^2} \sum_i C_i O_i + \text{H.c.} \quad (40)$$

In our case, the relevant operators are

$$O_9^{bs\ell\ell} = (\bar{s}\gamma_\alpha P_L b)(\bar{\ell}\gamma^\alpha \ell), \quad (41)$$

$$O_{10}^{bs\ell\ell} = (\bar{s}\gamma_\alpha P_L b)(\bar{\ell}\gamma^\alpha \gamma_5 \ell), \quad (42)$$

with $\ell \in \{e, \mu\}$.

Starting from the top quark operators $Q_{\ell\ell tt}^{\text{LR}}$, $Q_{\ell\ell ct}^{\text{LR}}$, $Q_{\ell\ell tt}^{\text{RR}}$, and $Q_{\ell\ell ct}^{\text{RR}}$, one-loop corrections from the weak interactions induce the $O_9^{bs\ell\ell}$ and $O_{10}^{bs\ell\ell}$ operators through diagrams such as the one shown in Fig. 1. We find for the corresponding Wilson coefficients

$$C_9^{bs\ell\ell} = \left(C_{\ell\ell tt}^{\text{RR}} + C_{\ell\ell tt}^{\text{LR}} + \frac{V_{cs}^*}{V_{ts}^*} \frac{m_c}{m_t} (C_{\ell\ell ct}^{\text{RR}} + C_{\ell\ell ct}^{\text{LR}}) \right)$$
$$\times \frac{1}{4s_W^2} \frac{m_t^2}{4m_W^2} \frac{v^2}{\Lambda^2} \log\left(\frac{\Lambda^2}{m_W^2}\right), \quad (43)$$
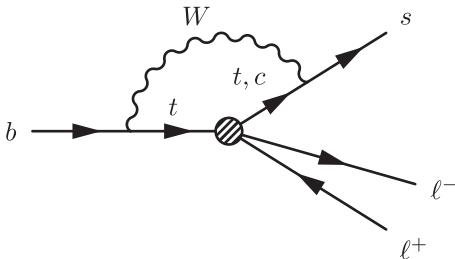
$$C_{10}^{bs\ell\ell} = \left(C_{\ell\ell tt}^{\text{RR}} - C_{\ell\ell tt}^{\text{LR}} + \frac{V_{cs}^*}{V_{ts}^*} \frac{m_c}{m_t} (C_{\ell\ell ct}^{\text{RR}} - C_{\ell\ell ct}^{\text{LR}}) \right)$$
$$\times \frac{1}{4s_W^2} \frac{m_t^2}{4m_W^2} \frac{v^2}{\Lambda^2} \log\left(\frac{\Lambda^2}{m_W^2}\right). \quad (44)$$

FIG. 1. Example of a Feynman diagram contributing to the rare decay $b \to s\ell^+\ell^-$.

The pieces proportional to $C_{\ell\ell tt}^{\text{LR}}$, $C_{\ell\ell tt}^{\text{RR}}$ have also been considered in Refs. [93–95] (see also Refs. [96–99] for related studies of B decay constraints on top operators). Note that we only take into account the logarithmically enhanced terms. Additional finite contributions from integrating out the top and W are renormalization-scheme dependent and of the same order as unknown matching contributions at the scale Λ. Therefore, they are consistently neglected in our study.

The Wilson coefficients $C_9^{bs\ell\ell}$ and $C_{10}^{bs\ell\ell}$ are probed at the $\mathcal{O}(1)$ level by existing data on rare B decays. (See e.g. the global fit in Ref. [100].) For several years, global fits found a strong preference for nonstandard values of some of the Wilson coefficients due to a series of "B-anomalies," notably the hints for lepton flavor universality violation in rare B decays through the observables R_K and R_{K^*} [101–104], anomalous angular observables in the $B \to K^*\mu\mu$ decay [105], and several anomalously low branching ratios of rare B decays [106–108]. Top-philic new physics has been discussed, e.g., in Refs. [94,95,109–113] as a possible explanation of the B anomalies.

However, the most recent updates on R_K and R_{K^*} [114,115] and the $B_s \to \mu^+\mu^-$ branching ratio [116] are in good agreement with SM predictions. We use these results to constrain new physics in the Wilson coefficients $C_9^{bs\ell\ell}$ and $C_{10}^{bs\ell\ell}$, see also [79,117].

We perform a fit including the following set of experimental results: (i) the world average of the $B_s \to \mu^+\mu^-$ branching ratio from HFLAV [118]; (ii) the new LHCb results on R_K and R_{K^*} [114,115]; (iii) the LHCb results on R_{K_S} and $R_{K^{*+}}$ [103]; (iv) the Belle results on LFU tests in $b \to s\ell\ell$ [119–121]. The corresponding theory predictions are obtained with FLAVIO [122] [version 2.3.3]. Instead of FLAVIO's default values for the CKM matrix elements we use the current PDG values, $|V_{cb}| = (40.8 \pm 1.4) \times 10^{-3}$ and $|V_{ub}| = (3.82 \pm 0.20) \times 10^{-3}$ [123]. Considering either muon-specific or electron-specific Wilson coefficients, the fit gives approximately

$$C_9^{bs\mu\mu} = -0.26 \pm 0.33, \qquad C_{10}^{bs\mu\mu} = -0.06 \pm 0.22, \quad (45)$$

with an error correlation of $\rho = 87\%$, and

$$C_9^{bsee} = 0.61 \pm 0.67, \qquad C_{10}^{bsee} = 0.43 \pm 0.73, \quad (46)$$

with an error correlation of $\rho = 97.7\%$. All new physics Wilson coefficients are compatible with zero at the 1σ level.

The above results can be translated into constraints on the flavor-conserving top quark coefficients C_{eett}^{RR}, C_{eett}^{LR}, $C_{\mu\mu tt}^{\text{RR}}$, and $C_{\mu\mu tt}^{\text{LR}}$. We find

$$\frac{-1}{(3.7\text{ TeV})^2} < \frac{C_{eett}^{\text{LR}}}{\Lambda^2} < \frac{1}{(1.2\text{ TeV})^2},$$

$$\frac{-1}{(0.80\text{ TeV})^2} < \frac{C_{eett}^{\text{RR}}}{\Lambda^2} < \frac{1}{(0.29\text{ TeV})^2},$$

$$\frac{-1}{(1.4\text{ TeV})^2} < \frac{C_{\mu\mu tt}^{\text{LR}}}{\Lambda^2} < \frac{1}{(2.6\text{ TeV})^2},$$

$$\frac{-1}{(0.95\text{ TeV})^2} < \frac{C_{\mu\mu tt}^{\text{RR}}}{\Lambda^2} < \frac{1}{(0.85\text{ TeV})^2}. \qquad (47)$$

In contrast to the constraints discussed in previous sections, the new physics contributions to the rare B decays are loop-induced and therefore contain a logarithmic dependence on the new physics scale Λ. The above best-fit ranges for the ratio of Wilson coefficients and new physics scale are derived setting the new physics Wilson coefficients $|C_{eett}^{\text{LR}}| = 1$, $|C_{eett}^{\text{RR}}| = 1$, $|C_{\mu\mu tt}^{\text{LR}}| = 1$, or $|C_{\mu\mu tt}^{\text{RR}}| = 1$, one at a time. As the bounds are based on a leading logarithmic analysis, they hold to very good approximation also for other values of the Wilson coefficients, as long as the Wilson coefficients are not parametrically different from one.

Turning to the flavor changing coefficients C_{eect}^{LR}, C_{eect}^{RR}, $C_{\mu\mu ct}^{\text{LR}}$, and $C_{\mu\mu ct}^{\text{RR}}$, we note that they can in principle be complex, and the respective bounds will depend on their complex phase. In most cases, the constraints on the imaginary parts of the Wilson coefficients are a factor of few weaker than the constraints on the real parts [100]. For simplicity, we will assume that the flavor-changing Wilson coefficients are real, and we will also neglect the tiny imaginary part of V_{ts} that enters Eqs. (43) and (44). Switching on only one of the flavor-changing coefficients C_{eect}^{LR}, C_{eect}^{RR}, $C_{\mu\mu ct}^{\text{LR}}$, $C_{\mu\mu ct}^{\text{RR}}$ at a time, the corresponding best-fit ranges for the new physics scale are somewhat smaller than the ones corresponding to the flavor conserving coefficients, and they can be obtained from Eq. (47) by rescaling with a factor $\sqrt{|V_{ts}/V_{cs}|}\sqrt{m_t/m_c} \simeq 3$.

Rare B decays could also be used to constrain the lepton-flavor-violating four-fermion operators [124], but we will not consider such processes in this work.

2. Decays of the Z boson

The decays of the Z boson to SM fermions have been measured with permille level precision at LEP. The good agreement with SM predictions gives stringent constraints on many new physics scenarios [125]. The new physics contact interactions that we consider in this work induce modifications of the Z decays to charged leptons, neutrinos, and quarks, through diagrams such as the one shown in Fig. 2.

We parametrize the new-physics effects in Z decays as modifications to the effective Z-fermion couplings. That is, we write
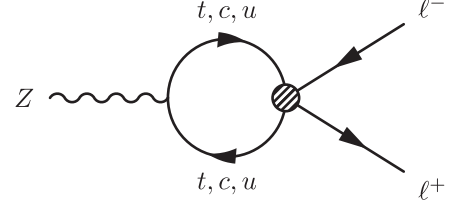

FIG. 2. Feynman diagram for a new physics contribution to the decay $Z \to \ell^+\ell^-$. The corresponding Feynman diagrams for $Z \to \nu\bar{\nu}$ and $Z \to q\bar{q}$ can be obtained by an appropriate replacement of quark and lepton lines.

$$\mathcal{L} \supset -\frac{g}{2c_W} Z_\mu[(g_L^f + \delta g_L^f)\bar{f}_L\gamma^\mu f_L + (g_R^f + \delta g_R^f)\bar{f}_R\gamma^\mu f_R], \qquad (48)$$

where $g_{L,R}^f$ are the SM Z couplings and the $\delta g_{L,R}^f$ are new-physics contributions. Using the above normalization, the SM couplings are given by

$$g_L^u = 1 - \frac{4}{3}s_W^2, \qquad g_L^\nu = 1, \qquad g_L^\ell = -1 + 2s_W^2,$$

$$g_R^u = -\frac{4}{3}s_W^2, \qquad g_R^\nu = 0, \qquad g_R^\ell = 2s_W^2 \qquad (49)$$

for up-type quarks, neutrinos, and charged leptons, respectively. The down-type couplings remain SM-like in our new physics scenarios and are therefore not considered in the following.

For the new physics contributions to the charged lepton couplings, we find

$$\delta g_X^\ell = -\left(\frac{3}{8\pi^2}\frac{m_t^2}{\Lambda^2} - \frac{s_W^2}{6\pi^2}\frac{m_Z^2}{\Lambda^2}\right)C_{\ell\ell tt}^{\text{XR}}\log\left(\frac{\Lambda^2}{m_t^2}\right) \\ + \frac{s_W^2}{6\pi^2}\frac{m_Z^2}{\Lambda^2}(C_{\ell\ell uu}^{\text{XR}} + C_{\ell\ell cc}^{\text{XR}})\log\left(\frac{\Lambda^2}{m_Z^2}\right), \qquad (50)$$

where $X \in \{L, R\}$ and $\ell \in \{e, \mu\}$. As in the case of the rare B decays discussed in the previous section, we consider the leading logarithmically enhanced new physics contributions and consistently neglect additional scheme-dependent terms. The Z couplings to left-handed neutrinos are shifted by

$$\delta g_L^{\nu_\ell} = -\left(\frac{3}{8\pi^2}\frac{m_t^2}{\Lambda^2} - \frac{s_W^2}{6\pi^2}\frac{m_Z^2}{\Lambda^2}\right)C_{\ell\ell tt}^{\text{LR}}\log\left(\frac{\Lambda^2}{m_t^2}\right) \\ + \frac{s_W^2}{6\pi^2}\frac{m_Z^2}{\Lambda^2}(C_{\ell\ell uu}^{\text{LR}} + C_{\ell\ell cc}^{\text{LR}})\log\left(\frac{\Lambda^2}{m_Z^2}\right), \qquad (51)$$

and the couplings to right-handed up-type quarks are shifted by

$$\delta g_{\mathrm{R}}^q = [(1 - 2s_W^2)(C_{eeqq}^{\mathrm{LR}} + C_{\mu\mu qq}^{\mathrm{LR}}) - 2s_W^2(C_{eeqq}^{\mathrm{RR}} + C_{\mu\mu qq}^{\mathrm{RR}})]\frac{s_W^2}{24\pi^2}\frac{m_Z^2}{\Lambda^2}\log\left(\frac{\Lambda^2}{m_Z^2}\right), \tag{52}$$

where $q \in \{u, c\}$. These modifications to the Z couplings lead to deviations of the Z partial widths from their SM predictions. For decays to charged leptons, we find

$$\frac{\Gamma(Z \to \ell\ell)}{\Gamma(Z \to \ell\ell)_{\mathrm{SM}}} = 1 + \frac{(1 - 2s_W^2)C_{\ell\ell tt}^{\mathrm{LR}} - 2s_W^2 C_{\ell\ell tt}^{\mathrm{RR}}}{1 - 4s_W^2 + 8s_W^4}\left(\frac{3}{4\pi^2}\frac{m_t^2}{\Lambda^2} - \frac{s_W^2}{3\pi^2}\frac{m_Z^2}{\Lambda^2}\right)\log\left(\frac{\Lambda^2}{m_t^2}\right)$$
$$+ \frac{(2s_W^2 - 1)(C_{\ell\ell uu}^{\mathrm{LR}} + C_{\ell\ell cc}^{\mathrm{LR}}) + 2s_W^2(C_{\ell\ell uu}^{\mathrm{RR}} + C_{\ell\ell cc}^{\mathrm{RR}})}{1 - 4s_W^2 + 8s_W^4}\frac{s_W^2}{3\pi^2}\frac{m_Z^2}{\Lambda^2}\log\left(\frac{\Lambda^2}{m_Z^2}\right). \tag{53}$$

Similarly, for the sum of the decay widths into neutrinos, we find

$$\frac{\Gamma(Z \to \nu\nu)}{\Gamma(Z \to \nu\nu)_{\mathrm{SM}}} = 1 - \frac{1}{3}(C_{eett}^{\mathrm{LR}} + C_{\mu\mu tt}^{\mathrm{LR}})\left(\frac{3}{4\pi^2}\frac{m_t^2}{\Lambda^2} - \frac{s_W^2}{3\pi^2}\frac{m_Z^2}{\Lambda^2}\right)\log\left(\frac{\Lambda^2}{m_t^2}\right)$$
$$+ \frac{1}{3}(C_{eeuu}^{\mathrm{LR}} + C_{\mu\mu uu}^{\mathrm{LR}} + C_{eecc}^{\mathrm{LR}} + C_{\mu\mu cc}^{\mathrm{LR}})\frac{s_W^2}{3\pi^2}\frac{m_Z^2}{\Lambda^2}\log\left(\frac{\Lambda^2}{m_Z^2}\right). \tag{54}$$

For the decay into an up-type quark-antiquark pair, we find

$$\frac{\Gamma(Z \to qq)}{\Gamma(Z \to qq)_{\mathrm{SM}}} = 1 + \frac{s_W^2}{\pi^2}\frac{m_Z^2}{\Lambda^2}\log\left(\frac{\Lambda^2}{m_Z^2}\right)\frac{(2s_W^2 - 1)(C_{eeqq}^{\mathrm{LR}} + C_{\mu\mu qq}^{\mathrm{LR}}) + 2s_W^2(C_{eeqq}^{\mathrm{RR}} + C_{\mu\mu qq}^{\mathrm{RR}})}{9 - 24s_W^2 + 32s_W^4}, \tag{55}$$

where $q \in \{u, c\}$. The decay widths into down-type quarks remain SM-like.

To obtain bounds on the Wilson coefficients entering Eqs. (53) to (55) above, we use the SM predictions and the LEP measurements of the Z partial widths given in Ref. [126] (Tables G.2 and 7.1, respectively). Considering one operator at a time, we find the bounds shown in Table II. The bounds hold as long as the Wilson coefficients are of $\mathcal{O}(1)$.

TABLE II. Lower bounds on Λ in TeV units from Z partial width measurements. Each row corresponds to a bound of the form $-1/\Lambda_-^2 < C/\Lambda^2 < 1/\Lambda_+^2$, with all other coefficients set to zero. In rows with multiple Wilson coefficients, the bound is the same for any of these coefficients set to 1 with the others set to zero. For the entries left empty, and for Wilson coefficients not shown in this table, there is no bound in the regime of validity of the EFT, i.e., with $\Lambda \gg m_Z$.

Final state	Coefficients	Λ_-	Λ_+
e^+e^-	C_{eett}^{LR}	1.6	2.3
	C_{eett}^{RR}	2.1	1.5
	$C_{eeuu}^{\mathrm{LR}}, C_{eecc}^{\mathrm{LR}}$	0.2	
	$C_{eeuu}^{\mathrm{RR}}, C_{eecc}^{\mathrm{RR}}$		0.2
$\mu^+\mu^-$	$C_{\mu\mu tt}^{\mathrm{LR}}$	1.5	1.5
	$C_{\mu\mu tt}^{\mathrm{RR}}$	1.4	1.4

3. Møller scattering

The MOLLER experiment [127] will measure the parity-violating asymmetry A_{PV} in polarized electron–electron scattering and determine the weak mixing angle at low energies with unprecedented precision. The asymmetry is defined by

$$A_{\mathrm{PV}} = \frac{\sigma_{\mathrm{L}} - \sigma_{\mathrm{R}}}{\sigma_{\mathrm{L}} + \sigma_{\mathrm{R}}}, \tag{56}$$

where σ_{L} (σ_{R}) refers to the cross section of left-handed (right-handed) polarized electrons scattering on fixed target electrons. From the point of view of a low-energy EFT, the asymmetry is induced by the parity-violating four-electron operator

$$\mathcal{L} \supset \frac{C_{\mathrm{Møller}}}{\Lambda^2}(\bar{e}\gamma^\mu\gamma_5 e)(\bar{e}\gamma_\mu e). \tag{57}$$

In the Standard Model, this operator can arise from tree-level Z boson exchange, but it is suppressed by the accidentally small vector coupling of the Z to electrons, proportional to $1 - 4s_W^2 \simeq 0.0744$ [128]. Precision measurements of A_{PV} are thus sensitive to new physics contributions to the operator in Eq. (57).

The flavor-conserving $(ee)(qq)$ operators that we consider in this work contribute to $C_{\mathrm{Møller}}$ at the one-loop level through diagrams as the one shown in Fig. 3. From a direct one-loop calculation, we find the following logarithmically enhanced terms:
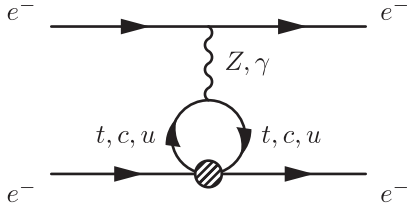
FIG. 3. Example new physics contribution to the Møller scattering amplitude at one loop.

$$
\begin{aligned}
\frac{C_{\text{Møller}}}{\Lambda^2} = \frac{G_F}{\sqrt{2}} \Bigg[& \frac{3}{8\pi^2} \frac{m_t^2}{\Lambda^2} C_{eett}^{\text{LR}} \log\left(\frac{\Lambda^2}{m_t^2}\right) \\
& + \left(\frac{3 s_W^2}{4\pi^2} \frac{m_t^2}{\Lambda^2} + \frac{s_W^2}{3\pi^2} \frac{m_W^2}{\Lambda^2}\right) (C_{eett}^{\text{RR}} - C_{eett}^{\text{LR}}) \log\left(\frac{\Lambda^2}{m_t^2}\right) \\
& + \frac{s_W^2}{3\pi^2} \frac{m_W^2}{\Lambda^2} \sum_{q=u,c} (C_{eeqq}^{\text{RR}} - C_{eeqq}^{\text{LR}}) \log\left(\frac{\Lambda^2}{m_q^2}\right) \Bigg].
\end{aligned} \tag{58}
$$

As in the other loop-induced processes discussed above, we consistently neglect additional nonlogarithmic terms. Note that in the up quark contribution ($q = u$), the quark mass in the logarithm should be replaced with an appropriate hadronic scale, e.g. $m_u^2 \to m_\pi^2 \simeq (140 \text{ MeV})^2$. We cross-checked the above result using the known anomalous dimensions of dimension-six operators in the Standard Model EFT and the low energy EFT below the electroweak scale [129–132].

The correction to the parity-violating asymmetry in Møller scattering that corresponds to the above Wilson coefficient can be written in the following way:

$$
\frac{\delta A_{\text{PV}}}{A_{\text{PV}}^{\text{SM}}} = \frac{2}{1 - 4s_W^2 + \Delta Q_W^e} \frac{\sqrt{2}}{G_F} \frac{C_{\text{Møller}}}{\Lambda^2}, \tag{59}
$$

where we include higher-order electroweak corrections to the SM prediction, $\Delta Q_W^e \simeq -0.0249$ [128,133].

The MOLLER experiment aims at a percent-level uncertainty, $|\delta A_{\text{PV}}|/A_{\text{PV}}^{\text{SM}} < 2.4\%$ [127], resulting in sensitivity to one-loop induced new physics at the TeV scale. More precisely, if one of the new physics operators is considered at a time, we find the following projected bounds:

$$
\begin{aligned}
&\frac{|C_{eett}^{\text{LR}}|}{\Lambda^2} < \frac{1}{(1.32 \text{ TeV})^2}, && \frac{|C_{eett}^{\text{RR}}|}{\Lambda^2} < \frac{1}{(1.36 \text{ TeV})^2}, \\
&\frac{|C_{eecc}^{\text{LR}}|}{\Lambda^2} < \frac{1}{(0.78 \text{ TeV})^2}, && \frac{|C_{eecc}^{\text{RR}}|}{\Lambda^2} < \frac{1}{(0.78 \text{ TeV})^2}, \\
&\frac{|C_{eeuu}^{\text{LR}}|}{\Lambda^2} < \frac{1}{(0.86 \text{ TeV})^2}, && \frac{|C_{eeuu}^{\text{RR}}|}{\Lambda^2} < \frac{1}{(0.86 \text{ TeV})^2}.
\end{aligned} \tag{60}
$$

Because the bounds are based on a leading logarithmic approximation of the one-loop contributions, they hold as long as the Wilson coefficients are of $\mathcal{O}(1)$. We note that in

our setup these expected sensitivities are weaker (stronger) than the existing constraints from Z decays in the case of operators involving top quarks (light quarks), see Table II.

V. NUMERICAL ANALYSIS

We now combine the theoretical constraints of Sec. III with the experimental constraints of Sec. IV to highlight constrained parameter space for both the Wilson coefficients and the observables themselves. In particular, if the sum rules in Eq. (12) hold, then experimental bounds on the flavor-conserving Wilson coefficients translate into restrictions on the flavor-violating coefficients. If observable data are eventually fitted to a region in the space of Wilson coefficients that violates the sum rules, this will imply one of the exceptional scenarios described in Sec. III, providing a wealth of information about the underlying UV physics.

We start by discussing a simple example for illustration. Consider the decays $t \to cee$ and $t \to uee$, assuming that they are induced by the Wilson coefficients C_{eect}^{RR} and C_{eeut}^{RR}, respectively. According to Eq. (12), these flavor-violating Wilson coefficients are bounded by the allowed sizes of the flavor-conserving C_{eett}^{RR}, C_{eecc}^{RR}, and C_{eeuu}^{RR}. In Sec. IV, we derived constraints on these flavor-conserving coefficients that in many cases remain strong even for values of Λ exceeding the TeV scale. The most stringent constraints on C_{eecc}^{RR} and C_{eeuu}^{RR} come from dilepton production at the LHC (see Table I) and read as follows:

$$
-\frac{1}{(8.8 \text{ TeV})^2} < \frac{C_{eeuu}^{\text{RR}}}{\Lambda^2} < \frac{1}{(5.9 \text{ TeV})^2}, \tag{61}
$$

$$
-\frac{1}{(2.0 \text{ TeV})^2} < \frac{C_{eecc}^{\text{RR}}}{\Lambda^2} < \frac{1}{(2.0 \text{ TeV})^2}. \tag{62}
$$

The strongest constraint on C_{eett}^{RR} is from the LEP precision measurements of Z decays (see Table II), leading to

$$
-\frac{1}{(2.1 \text{ TeV})^2} < \frac{C_{eett}^{\text{RR}}}{\Lambda^2} < \frac{1}{(1.5 \text{ TeV})^2}. \tag{63}
$$

The current experimental constraints on the corresponding flavor-violating Wilson coefficients, however, correspond to $\Lambda < 1$ TeV, per Eqs. (16) and (17). Thus, the theoretical constraints provide a new, stronger bound. In this example, the sum rules imply

$$
\frac{|C_{eeut}^{\text{RR}}|}{\Lambda^2} < \frac{1}{(3.0 \text{ TeV})^2}, \qquad \frac{|C_{eect}^{\text{RR}}|}{\Lambda^2} < \frac{1}{(1.7 \text{ TeV})^2}, \tag{64}
$$

which are indeed much more stringent than the direct experimental bounds in Eqs. (16) and (17). This translates into the following upper bounds on rare top decay branching ratios:

$$BR(t \to ce^+e^-) \lesssim 3 \times 10^{-7}, \qquad (65)$$

$$BR(t \to ue^+e^-) \lesssim 3 \times 10^{-8}. \qquad (66)$$

Future observation of the rare top decays above these target values would exclude the full class of new physics models that can be described by the Wilson coefficients C_{eect}^{RR}, C_{eeut}^{RR}, C_{eett}^{RR}, C_{eecc}^{RR}, and C_{eeuu}^{RR} and that obey the sum rules in Eq. (12). Note that the targets in Eqs. (65) and (66) are 3–4 orders of magnitude below the current direct bounds on the branching ratios given in Eq. (15), leaving ample parameter space to be probed.

Following the pattern of this example, we now explore the implications of the sum rules in a systematic way. First, we consider the implications of the sum rules for the Wilson coefficients themselves. In general, each sum rule determines a region in a parameter space with five real degrees of freedom: the EFT scale Λ, two real flavor-conserving Wilson coefficients, and one complex flavor-violating Wilson coefficient. We show two-dimensional slices through this parameter space determined by the following conditions:

(1) The EFT scale Λ is fixed to a single value.
(2) We vary one flavor-conserving and one flavor-violating Wilson coefficient, restricting the flavor-violating coefficient to be real and positive.
(3) The second flavor-conserving coefficient is set to its largest value compatible with experimental bounds with all other coefficients set to zero. This leads to the most conservative form of the sum rules (i.e., the least stringent theoretical bound on the flavor violating Wilson coefficients).
(4) We impose perturbativity, requiring $|C_{abcd}| < 4\pi$ for all Wilson coefficients. This is required in order to self-consistently relate the Wilson coefficients to observables.

The constrained regions are shown in Fig. 4 for the case of the LR operator with c–t flavor violation coupled to left-handed electrons. For completeness, other cases are qualitatively very similar and shown in Fig. 6. The sum rules are always violated for sufficiently large values of the flavor-violating coefficient, indicating that the measurement of a single flavor-violating observable can diagnose the failure of the sum rules to apply.

The sum rules also impose restrictions in the space of observables: that is, there exist points in the space of observables that cannot be produced by any combination of perturbative Wilson coefficients satisfying the sum rules. Thus, if future experimental data were to prefer such a point, this would imply either one of the exceptional scenarios discussed in Sec. III or a nonperturbative theory.

To locate such points, we take a purely numerical approach: we sample the space of Wilson coefficients with a set of points $\{\mathbf{C}_i\}$ and discard all points that are inconsistent with experimental bounds at 95% CL. We repeat the process including only samples that satisfy the sum rules, producing a set of points $\{\mathbf{C}_i^{SR}\}$. Each point $\mathbf{C}_i$ in the space of Wilson coefficients maps to a point $\mathbf{O}_i$ in the space of observables, so we obtain two corresponding sets of points $\{\mathbf{O}_i\}$ and $\{\mathbf{O}_i^{SR}\}$ in observable space. From these points, we determine regions R and $R^{SR} \subset R$ in observable
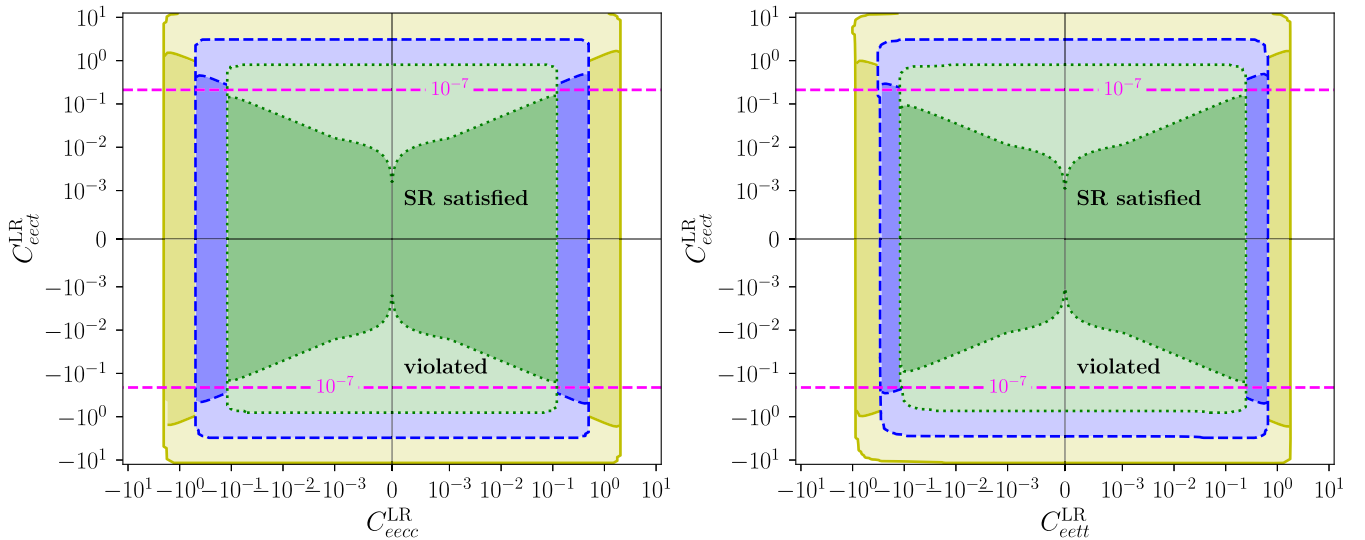

FIG. 4. Implications of the sum rules for the Wilson coefficients. In the left (right) panel, $C_{\ell\ell tt}^{LR}$ ($C_{\ell\ell cc}^{LR}$) is fixed to its maximum value consistent with experimental bounds and perturbativity. The green, blue, and yellow regions correspond to $\Lambda = 500$ GeV, 1 TeV, 2 TeV. For each color, the darker shaded region is consistent with sum rules for some allowed value of the suppressed coefficient. The light shaded regions are inconsistent with experimental data if sum rules are imposed. Note that the regions corresponding to higher Λ are partially obscured by those corresponding to lower Λ. The dashed magenta line shows the contour $BR(t \to ce^+e^-) = 10^{-7}$ for $\Lambda = 1$ TeV, corresponding to the blue region.

space that are compatible with observables and additionally compatible with the sum rules. In the limit of a large number of sample points, the region $R \backslash R^{\mathrm{SR}}$ consists of points in observable space that are consistent with data but inconsistent with the sum rules in the space of Wilson coefficients.

We carry out the sampling using the Metropolis–Hastings algorithm, taking the target probability density to be proportional to $\|\mathbf{O}\| \exp(-\chi^2(\Lambda, \mathbf{C})/\chi^2_{\mathrm{cut}})$, where $\mathbf{C}$ denotes the Wilson coefficients, $\chi^2(\Lambda, \mathbf{C})$ denotes the associated chi-square test statistic, $\mathbf{O}$ denotes the point in the plane of observables, and χ^2_{cut} is a constant cutoff. This functional form is chosen to ensure an enhanced sampling probability for points that are in tension with experiments, in order to fully sample the boundaries of R and R^{SR}. Note that after imposing perturbativity, the space of Wilson coefficients is bounded, so it is also possible to

sample the space exhaustively. While this approach is inefficient, we have performed log-uniform sampling to check that the results are qualitatively similar to those obtained with the Metropolis–Hastings approach.

In the numerical sampling, we include complex phases for flavor-violating coefficients, and we vary both C^{LR}_{abcd} and C^{RR}_{abcd}. We show results for electronic observables, and neglect any coupling to muons. In addition to the Wilson coefficients, we simultaneously vary the new physics scale Λ over a bounded domain: to accord with experimental constraints and capabilities, we impose 100 GeV $< \Lambda <$ 100 TeV.

We show the results of this computation in two-dimensional slices through the space of observables in Fig. 5. To demonstrate the most nontrivial structures, we pair the flavor-violating observable $\mathrm{BR}(t \to c\bar{e}^+e^-)$ with flavor-conserving observables. For example, the top-left panel shows the regions R (light blue) and R^{SR} (light orange) in the
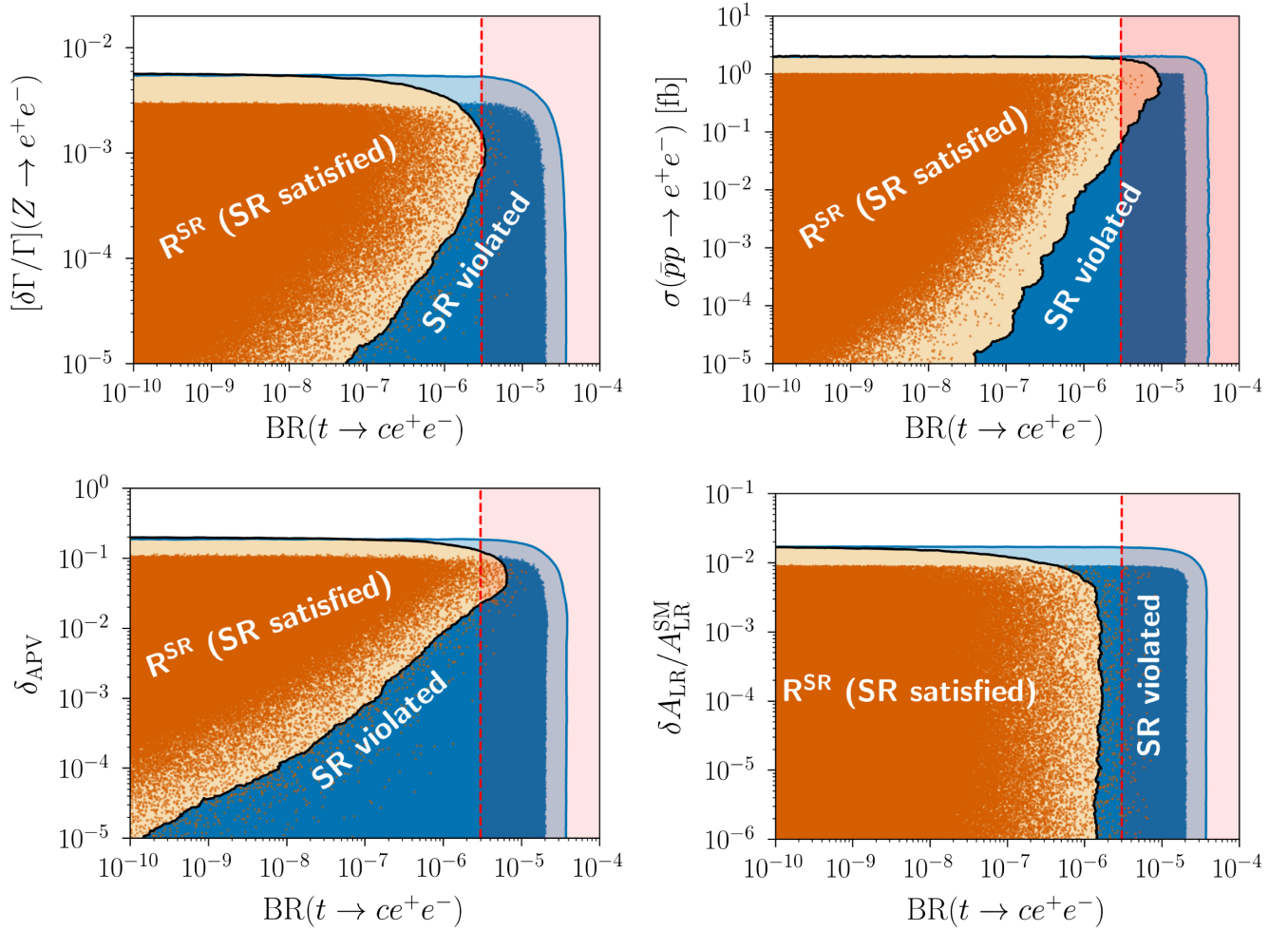

FIG. 5. Allowed regions with sample points in planes of complementary observables with 100 GeV $< \Lambda <$ 100 TeV. All points are compatible with all the observables considered in this work. The orange points correspond to combinations of Wilson coefficients that satisfy the sum rules. The lighter shaded regions show the regions R (orange) and R^{SR} (blue), determined as described in the text. The red regions indicate parameter space that will be constrained by expected experimental searches of $\mathrm{BR}(t \to c e^+e^-)$ [7]. In particular, almost any nonzero measurement of $\mathrm{BR}(t \to c e^+e^-)$ in the upcoming generation of experiments (see dashed red line in the figure) would likely be incompatible with the sum rules under the assumptions made here.
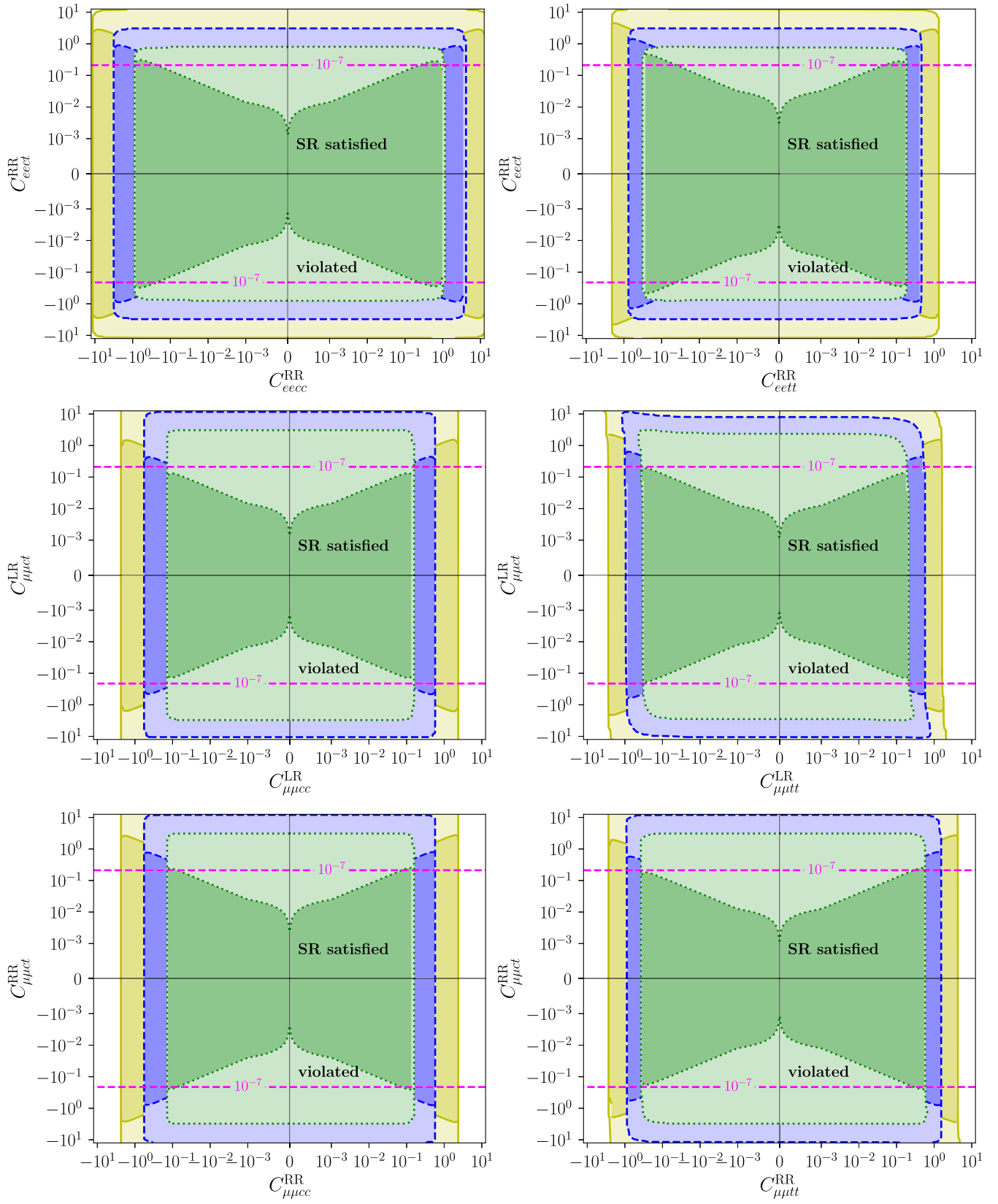
FIG. 6. Implications of the sum rules, as in Fig. 4, for additional pairs of Wilson coefficients.

plane of the branching ratio $BR(t \to ce^+e^-)$ and the decay width of the Z boson to electrons $\Gamma(Z \to \bar{e}e)$, with the latter shown as the fractional shift from the SM value. The actual points sampled are shown in dark blue and dark orange. The difference between R and R^{SR} consists of points that are inconsistent with either the sum rules or the bounds imposed on the Wilson coefficients and new physics scale.

Here, a sufficiently large value of the flavor-violating observable $BR(t \to c\bar{e}e)$ always implies violation of the sum rules due to the experimental bounds on the corresponding flavor-conserving Wilson coefficients. For smaller values of $BR(t \to c\bar{e}e)$, consistency with the sum rules imposes a restriction on $\Gamma(Z \to \bar{e}e)$. The red region bounded by the red dashed line in each plot indicates the expected future sensitivity to the flavor-violating top branching ratio estimated in Ref. [7], which arises from a phenomenological recasting of a ATLAS search for $t \to Zq$. All in all, the sum rules together with the experimental bounds on flavor conserving operators imply an upper bound on the branching ratio of $t \to ce^+e^-$ roughly an order of magnitude more stringent than the present experimental bound on the branching ratio.

Translating a discrete set of sample points to continuous regions R and R^{SR} requires a prescription for determining the inclusion of arbitrary points in the plane. In Fig. 5, we include a test point p in a region if 100 sample points lie within a distance corresponding to a factor of 0.3 in each direction (i.e., within a ball of radius 0.3 in log space). This means that some small number of points satisfy the sum rules but nonetheless lie outside the region R^{SR} as shown. However, these points are extremely sparse, and reflect the fact that it is possible to evade our constraints with extreme tuning.

VI. CONCLUSIONS

The existence of the sum rules of Eq. (12) at dimension six relating flavor-conserving and flavor-violating quark–lepton operators has nontrivial consequences for low-energy BSM phenomenology, both for the viability of particular classes of models and for the interpretation of a BSM signal in future experiments. We now summarize the implications of these theoretical bounds for the experimental outlook.

Typically, theoretical bounds based on positivity and unitarity are invoked to rule out regions of parameter space, motivating searches in other regimes. With a few key assumptions, it is possible to set similar constraints with the sum rules considered in this work. In this case, Fig. 5 can be interpreted as theoretical constraints on observationally accessible new physics, given the following conditions:

(1) The sum rules hold, i.e., the assumptions in Sec. III are satisfied.
(2) Any new-physics couplings to muons can be neglected, a simplifying assumption made to reduce the dimensionality of the parameter space.

(3) The scale of new physics lies between 100 GeV and 100 TeV, such that BSM effects are observable but not already in frank conflict with observations.
(4) The new physics is perturbative, such that the contributions to observables can be reliably computed.

Given these assumptions, it is possible to make direct statements about observables. For example, in the absence of severe fine tuning, Fig. 5 implies that $BR(t \to c\bar{e}e) \lesssim 10^{-5}$, an order of magnitude below current experimental bounds.

However, the first assumption above is interestingly fragile: the sum rules fail to hold for some UV structures. In particular, the sum rules can be violated if the effective interactions arise from a combination of scalar and vector interactions in the UV, or if the forward scattering amplitude grows faster than s^1. Thus, rather than ruling out parameter space, the sum rules highlight parameter space where low-energy observables encode nontrivial features of the UV physics. The measurement of a combination of observables incompatible with the sum rules would immediately imply one of the alternative scenarios in Sec. III. Thus, rather than excluding parameter space, these constraints *motivate* experimental searches in sum rule–violating regimes.

The present work establishes the first such step toward establishing UV properties from low-energy observables: in particular, we have found that rare top decays provide the best observational prospects to probe the violation of the sum rules. If the sum rules hold, then the relationship between flavor-conserving and flavor-violating observables is substantially constrained. Indeed, any positive detection of flavor-violating top decays in the upcoming generation of experiments must signal a violation of the sum rules under the assumptions of this work. As indicated by the red bands in Fig. 5, upcoming experiments will not be sensitive to flavor-violating top decays in most of the parameter space consistent with the sum rules in the absence of an extreme fine-tuning. Thus, ongoing searches for flavor-violating top decays nontrivially probe the structure of UV physics. This is one of the main results of the present work.

In our numerical analysis we have focused on the flavor-violating process $t \to c\ell\ell$, which is poorly constrained by direct searches. However, similar results apply for e.g. $t \to u\ell\ell$. Extensions of the theoretical constraints used in this paper may give rise to additional targets elsewhere in the parameter space. Beyond the opportunities to exploit other sum rules in a similar context, we note that we have considered only quark flavor violation. Lepton flavor violation would provide an alternative set of observables that may allow for complementary tests of the sum rules. The use of theoretical constraints may prove especially important for the program of global fits of large numbers of SMEFT coefficients to all available data (see, e.g., [5,20,22,25]). In particular, such global fits may give substantially different results with or without these sum rules as a prior constraint, which further motivates experimental searches along these lines.

TABLE III. Summary of all bounds on the EFT scale Λ in TeV units. Each row corresponds to a bound of the form $-1/\Lambda_-^2 < C/\Lambda^2 < 1/\Lambda_+^2$, where C denotes the Wilson coefficient in question. For the entries left empty, and for Wilson coefficients not shown in this table, there is no bound in the regime of validity of the EFT, i.e., with $\Lambda \gg m_Z$.

Coefficient	Λ_-	Λ_+	Coefficient	Λ_-	Λ_+
Rare t decays			*Rare t decays*		
C_{eect}^{LR}	0.32	0.32	C_{eect}^{RR}	0.32	0.32
C_{eeut}^{LR}	0.33	0.33	C_{eeut}^{RR}	0.33	0.33
$C_{\mu\mu ct}^{LR}$	0.35	0.35	$C_{\mu\mu ct}^{RR}$	0.35	0.35
$C_{\mu\mu ut}^{LR}$	0.36	0.36	$C_{\mu\mu ut}^{RR}$	0.36	0.36
$C_{\mu etc}^{LR}$	1.1	1.1	$C_{\mu etc}^{RR}$	1.1	1.1
$C_{e\mu tc}^{LR}$	1.1	1.1	$C_{e\mu tc}^{RR}$	1.1	1.1
$C_{\mu etu}^{LR}$	2.0	2.0	$C_{\mu etu}^{RR}$	2.0	2.0
$C_{e\mu tu}^{LR}$	2.0	2.0	$C_{e\mu tu}^{RR}$	2.0	2.0
Single t production			*Single t production*		
C_{eect}^{LR}	0.70	0.70	C_{eect}^{RR}	0.70	0.70
C_{eeut}^{LR}	0.70	0.70	C_{eeut}^{RR}	0.70	0.70
Dilepton spectra			*Dilepton spectra*		
C_{eeuu}^{LR}	8.0	6.5	$C_{\mu\mu uu}^{LR}$	8.0	5.9
C_{eeuu}^{RR}	8.8	5.9	$C_{\mu\mu uu}^{RR}$	9.2	5.1
C_{eecc}^{LR}	2.0	2.0	$C_{\mu\mu cc}^{LR}$	2.1	2.0
C_{eecc}^{RR}	2.0	2.0	$C_{\mu\mu cc}^{RR}$	2.1	2.0
Rare B decays			*Rare B decays*		
C_{eett}^{LR}	3.7	1.2	C_{eett}^{RR}	0.80	0.29
$C_{\mu\mu tt}^{LR}$	1.4	2.6	$C_{\mu\mu tt}^{RR}$	0.95	0.85
Z decays			*Z decays*		
C_{eett}^{LR}	1.6	2.3	C_{eett}^{RR}	2.1	1.5
C_{eeuu}^{LR}	0.20		C_{eecc}^{LR}	0.20	
C_{eeuu}^{RR}		0.20	C_{eecc}^{RR}		0.20
$C_{\mu\mu tt}^{LR}$	1.5	1.5	$C_{\mu\mu tt}^{RR}$	1.4	1.4
Møller scattering (expected)			*Møller scattering* (expected)		
C_{eett}^{LR}	1.32	1.32	C_{eett}^{RR}	1.36	1.36
C_{eecc}^{LR}	0.78	0.78	C_{eecc}^{RR}	0.78	0.78
C_{eeuu}^{LR}	0.86	0.86	C_{eeuu}^{RR}	0.86	0.86
$^{12}C - e^-$ scattering (expected)			$p^+ - e^-$ scattering (expected)		
$C_{eeuu}^{RR} - C_{eeuu}^{LR}$	5.7	5.7	$C_{eeuu}^{RR} - C_{eeuu}^{LR}$	7.5	7.5
Atomic parity violation					
$C_{eeuu}^{RR} - C_{eeuu}^{LR}$	7.2	3.1			

[1] J. A. Aguilar-Saavedra, Top flavor-changing neutral interactions: Theoretical expectations and experimental detection, Acta Phys. Pol. B **35**, 2695 (2004).

[2] W. Altmannshofer, B. Maddock, and D. Tuckler, Rare top decays as probes of flavorful Higgs bosons, Phys. Rev. D **100**, 015003 (2019).

[3] B. Grzadkowski, M. Iskrzynski, M. Misiak, and J. Rosiek, Dimension-six terms in the standard model Lagrangian, J. High Energy Phys. 10 (2010) 085.

[4] J. Drobnak, S. Fajfer, and J. F. Kamenik, Signatures of NP models in top FCNC decay $t \to c(u)l^+l^-$, J. High Energy Phys. 03 (2009) 077.

[5] G. Durieux, F. Maltoni, and C. Zhang, Global approach to top-quark flavor-changing interactions, Phys. Rev. D **91**, 074017 (2015).

[6] M. Forslund and N. Kidonakis, Associated production of a top quark with a photon via anomalous couplings, Phys. Rev. D **98**, 074017 (2018).

[7] M. Chala, J. Santiago, and M. Spannowsky, Constraining four-fermion operators using rare top decays, J. High Energy Phys. 04 (2019) 014.

[8] L. Shi and C. Zhang, Probing the top quark flavor-changing couplings at CEPC, Chin. Phys. C **43**, 113104 (2019).

[9] Y. Afik, S. Bar-Shalom, A. Soni, and J. Wudka, New flavor physics in di- and trilepton events from single-top production at the LHC and beyond, Phys. Rev. D **103**, 075031 (2021).

[10] C. Degrande, J.-M. Gerard, C. Grojean, F. Maltoni, and G. Servant, Non-resonant new physics in top pair production at hadron colliders, J. High Energy Phys. 03 (2011) 125.

[11] C. Zhang and S. Willenbrock, Effective-field-theory approach to top-quark production and decay, Phys. Rev. D **83**, 034006 (2011).

[12] A. Buckley, C. Englert, J. Ferrando, D. J. Miller, L. Moore, M. Russell, and C. D. White, Constraining top quark effective theory in the LHC Run II era, J. High Energy Phys. 04 (2016) 015.

[13] M. Schulze and Y. Soreq, Pinning down electroweak dipole operators of the top quark, Eur. Phys. J. C **76**, 466 (2016).

[14] F. Maltoni, E. Vryonidou, and C. Zhang, Higgs production in association with a top-antitop pair in the Standard Model effective field theory at NLO in QCD, J. High Energy Phys. 10 (2016) 123.

[15] C. Degrande, F. Maltoni, K. Mimasu, E. Vryonidou, and C. Zhang, Single-top associated production with a Z or H boson at the LHC: The SMEFT interpretation, J. High Energy Phys. 10 (2018) 005.

[16] M. de Beurs, E. Laenen, M. Vreeswijk, and E. Vryonidou, Effective operators in t-channel single top production and decay, Eur. Phys. J. C **78**, 919 (2018).

[17] M. Farina, C. Mondino, D. Pappadopulo, and J. T. Ruderman, New physics from high energy tops, J. High Energy Phys. 01 (2019) 231.

[18] N. P. Hartland, F. Maltoni, E. R. Nocera, J. Rojo, E. Slade, E. Vryonidou, and C. Zhang, A Monte Carlo global analysis of the standard model effective field theory: The top quark sector, J. High Energy Phys. 04 (2019) 100.

[19] G. Durieux, A. Irles, V. Miralles, A. Peñuelas, R. Pöschl, M. Perelló, and M. Vos, The electro-weak couplings of the top and bottom quarks—Global fit and future prospects, J. High Energy Phys. 12 (2019) 098; 01 (2021) 195(E).

[20] I. Brivio, S. Bruggisser, F. Maltoni, R. Moutafis, T. Plehn, E. Vryonidou, S. Westhoff, and C. Zhang, O new physics, where art thou? A global search in the top sector, J. High Energy Phys. 02 (2020) 131.

[21] D. Stolarski and A. Tonero, Constraining new physics with single top production at LHC, J. High Energy Phys. 08 (2020) 036.

[22] J. Ellis, M. Madigan, K. Mimasu, V. Sanz, and T. You, Top, Higgs, diboson and electroweak fit to the standard model effective field theory, J. High Energy Phys. 04 (2021) 279.

[23] Y. Afik, S. Bar-Shalom, K. Pal, A. Soni, and J. Wudka, Multi-lepton probes of new physics and lepton-universality in top-quark interactions, Nucl. Phys. **B980**, 115849 (2022).

[24] V. Miralles, M. M. López, M. M. Llácer, A. Peñuelas, M. Perelló, and M. Vos, The top quark electro-weak couplings after LHC Run 2, J. High Energy Phys. 02 (2022) 032.

[25] J. J. Ethier, G. Magni, F. Maltoni, L. Mantani, E. R. Nocera, J. Rojo, E. Slade, E. Vryonidou, and C. Zhang (SMEFiT Collaboration), Combined SMEFT interpretation of Higgs, diboson, and top quark data from the LHC, J. High Energy Phys. 11 (2021) 089.

[26] Y. Liu, Y. Wang, C. Zhang, L. Zhang, and J. Gu, Probing top-quark operators with precision electroweak measurements, Chin. Phys. C **46**, 113105 (2022).

[27] R. K. Barman and A. Ismail, Constraining the top electroweak sector of the SMEFT through Z associated top pair and single top production at the HL-LHC, arXiv:2205.07912.

[28] A. Adams, N. Arkani-Hamed, S. Dubovsky, A. Nicolis, and R. Rattazzi, Causality, analyticity and an IR obstruction to UV completion, J. High Energy Phys. 10 (2006) 014.

[29] J. Distler, B. Grinstein, R. A. Porto, and I. Z. Rothstein, Falsifying Models of New Physics via WW Scattering, Phys. Rev. Lett. **98**, 041601 (2007).

[30] L. Vecchi, Causal versus analytic constraints on anomalous quartic gauge couplings, J. High Energy Phys. 11 (2007) 054.

[31] C. Zhang and S.-Y. Zhou, Positivity bounds on vector boson scattering at the LHC, Phys. Rev. D **100**, 095003 (2019).

[32] Q. Bi, C. Zhang, and S.-Y. Zhou, Positivity constraints on aQGC: Carving out the physical parameter space, J. High Energy Phys. 06 (2019) 137.

[33] G. N. Remmen and N. L. Rodd, Consistency of the standard model effective field theory, J. High Energy Phys. 12 (2019) 032.

[34] J. Ellis, H.-J. He, and R.-Q. Xiao, Probing new physics in dimension-8 neutral gauge couplings at e^+e^- colliders, Sci. China Phys. Mech. Astron. **64**, 221062 (2021).

[35] K. Yamashita, C. Zhang, and S.-Y. Zhou, Elastic positivity vs extremal positivity bounds in SMEFT: A case study in transversal electroweak gauge-boson scatterings, J. High Energy Phys. 01 (2021) 095.

[36] J. Ellis, S.-F. Ge, H.-J. He, and R.-Q. Xiao, Probing the scale of new physics in the $ZZ\gamma$ coupling at e^+e^- colliders, Chin. Phys. C **44,** 063106 (2020).

[37] J. Ellis, H.-J. He, and R.-Q. Xiao, Probing neutral triple gauge couplings at the LHC and future hadron colliders, Phys. Rev. D **107,** 035005 (2023).

[38] B. Bellazzini and F. Riva, New phenomenological and theoretical perspective on anomalous ZZ and $Z\gamma$ processes, Phys. Rev. D **98,** 095021 (2018).

[39] J. Gu, L.-T. Wang, and C. Zhang, Unambiguously Testing Positivity at Lepton Colliders, Phys. Rev. Lett. **129,** 011805 (2022).

[40] B. Fuks, Y. Liu, C. Zhang, and S.-Y. Zhou, Positivity in electron-positron scattering: Testing the axiomatic quantum field theory principles and probing the existence of UV states, Chin. Phys. C **45,** 023108 (2021).

[41] X. Li, K. Mimasu, K. Yamashita, C. Yang, C. Zhang, and S.-Y. Zhou, Moments for positivity: Using Drell-Yan data to test positivity bounds and reverse-engineer new physics, J. High Energy Phys. 10 (2022) 107.

[42] G. N. Remmen and N. L. Rodd, Flavor Constraints from Unitarity and Analyticity, Phys. Rev. Lett. **125,** 081601 (2020).

[43] Q. Bonnefoy, E. Gendy, and C. Grojean, Positivity bounds on minimal flavor violation, J. High Energy Phys. 04 (2021) 115.

[44] G. N. Remmen and N. L. Rodd, Signs, spin, SMEFT: Sum rules at dimension six, Phys. Rev. D **105,** 036006 (2022).

[45] A. Azatov, D. Ghosh, and A. H. Singh, Four-fermion operators at dimension 6: Dispersion relations and UV completions, Phys. Rev. D **105,** 115019 (2022).

[46] C. Zhang, SMEFTs living on the edge: Determining the UV theories from positivity and extremality, J. High Energy Phys. 12 (2022) 096.

[47] G. N. Remmen and N. L. Rodd, Spinning sum rules for the dimension-six SMEFT, J. High Energy Phys. 09 (2022) 030.

[48] P. J. Fox, Z. Ligeti, M. Papucci, G. Perez, and M. D. Schwartz, Deciphering top flavor violation at the LHC with B factories, Phys. Rev. D **78,** 054008 (2008).

[49] J. Davighi, S. Melville, and T. You, Natural selection rules: New positivity bounds for massive spinning particles, J. High Energy Phys. 02 (2022) 167.

[50] A. M. Sirunyan *et al.* (CMS Collaboration), Search for new physics in top quark production with additional leptons in proton-proton collisions at $\sqrt{s} = 13$ TeV using effective field theory, J. High Energy Phys. 03 (2021) 095.

[51] G. Aad *et al.* (ATLAS Collaboration), Search for new phenomena in events with an energetic jet and missing transverse momentum in pp collisions at $\sqrt{s} = 13$ TeV with the ATLAS detector, Phys. Rev. D **103,** 112006 (2021).

[52] A. Tumasyan *et al.* (CMS Collaboration), Search for new particles in events with energetic jets and large missing transverse momentum in proton-proton collisions at $\sqrt{s} = 13$ TeV, J. High Energy Phys. 11 (2021) 153.

[53] D. Akimov *et al.* (COHERENT Collaboration), Observation of coherent elastic neutrino-nucleus scattering, Science **357,** 1123 (2017).

[54] W. Altmannshofer, M. Tammaro, and J. Zupan, Nonstandard neutrino interactions and low energy experiments, J. High Energy Phys. 09 (2019) 083; 11 (2021) 113(E).

[55] M. Aaboud *et al.* (ATLAS Collaboration), Search for flavour-changing neutral current top-quark decays $t \to qZ$ in proton-proton collisions at $\sqrt{s} = 13$ TeV with the ATLAS detector, J. High Energy Phys. 07 (2018) 176.

[56] A. M. Sirunyan *et al.* (CMS Collaboration), Search for associated production of a Z boson with a single top quark and for tZ flavour-changing interactions in pp collisions at $\sqrt{s} = 8$ TeV, J. High Energy Phys. 07 (2017) 003.

[57] A. Abada *et al.* (FCC Collaboration), FCC physics opportunities: Future circular collider conceptual design report volume 1, Eur. Phys. J. C **79,** 474 (2019).

[58] S. Davidson, M. L. Mangano, S. Perries, and V. Sordini, Lepton flavour violating top decays at the LHC, Eur. Phys. J. C **75,** 450 (2015).

[59] C. A. Gottardo (ATLAS Collaboration), Search for charged lepton-flavour violation in top-quark decays at the LHC with the ATLAS detector, in *11th International Workshop on Top Quark Physics* (eConf, Bad Neuenahr, Germany, 2018), arXiv:1809.09048.

[60] A. Tumasyan *et al.* (CMS Collaboration), Search for charged-lepton flavor violation in top quark production and decay in pp collisions at $\sqrt{s} = 13$ TeV, J. High Energy Phys. 06 (2022) 082.

[61] Search for charged-lepton-flavour violating $\mu\tau qt$ interactions in top-quark production and decay with the ATLAS detector at the LHC (2023), https://cds.cern.ch/record/2845451?ln=en.

[62] S. Bar-Shalom and J. Wudka, Flavor changing single top quark production channels at e^+e^- colliders in the effective Lagrangian description, Phys. Rev. D **60,** 094016 (1999).

[63] R. Bause, H. Gisbert, M. Golz, and G. Hiller, Lepton universality and lepton flavor conservation tests with dineutrino modes, Eur. Phys. J. C **82,** 164 (2022).

[64] S. Sun, Q.-S. Yan, X. Zhao, and Z. Zhao, Constraining rare B decays by $\mu^+\mu^- \to tc$ at future lepton colliders, arXiv:2302.01143.

[65] CERN, Search for single top production via flavour changing neutral currents: Preliminary combined results of the LEP experiments, Report No. DELPHI-2001-119 CONF 542, 2001, https://cds.cern.ch/record/1006392.

[66] P. Achard *et al.* (L3 Collaboration), Search for single top production at LEP, Phys. Lett. B **549,** 290 (2002).

[67] J. Abdallah *et al.* (DELPHI Collaboration), Search for single top quark production via contact interactions at LEP2, Eur. Phys. J. C **71,** 1555 (2011).

[68] H. Cheng *et al.* (CEPC Physics Study Group), The physics potential of the CEPC. Prepared for the US Snowmass Community Planning Exercise (Snowmass 2021), in *2022 Snowmass Summer Study* (eConf, Seattle, 2022), arXiv:2205.08553.

[69] G. Bernardi *et al.*, The future circular collider: A summary for the US 2021 Snowmass process, arXiv:2203.06520.

[70] A. Aryshev *et al.* (ILC International Development Team), The International Linear Collider: Report to Snowmass 2021, (2022), arXiv:2203.07622.

[71] H. Al Ali *et al.*, The muon smasher's guide, Rep. Prog. Phys. **85,** 084201 (2022).

[72] F. D. Aaron *et al.* (H1 Collaboration), Search for single top quark production at HERA, Phys. Lett. B **678,** 450 (2009).

[73] H. Abramowicz *et al.* (ZEUS Collaboration), Search for single-top production in ep collisions at HERA, Phys. Lett. B **708,** 27 (2012).

[74] A. Greljo and D. Marzocca, High-p_T dilepton tails and flavor physics, Eur. Phys. J. C **77,** 548 (2017).

[75] G. Aad *et al.* (ATLAS Collaboration), Search for new non-resonant phenomena in high-mass dilepton final states with the ATLAS detector, J. High Energy Phys. 11 (2020) 005; 04 (2021) 142(E).

[76] A. M. Sirunyan *et al.* (CMS Collaboration), Search for resonant and nonresonant new phenomena in high-mass dilepton final states at $\sqrt{s} = 13$ TeV, J. High Energy Phys. 07 (2021) 208.

[77] L. Allwicher, D. A. Faroughy, F. Jaffredo, O. Sumensari, and F. Wilsch, Drell-Yan tails beyond the standard model, J. High Energy Phys. 03 (2023) 064.

[78] L. Allwicher, D. A. Faroughy, F. Jaffredo, O. Sumensari, and F. Wilsch, HighPT: A tool for high-p_T Drell-Yan tails beyond the standard model, arXiv:2207.10756.

[79] A. Greljo, J. Salko, A. Smolkovič, and P. Stangl, Rare b decays meet high-mass Drell-Yan, arXiv:2212.10497.

[80] L. A. Harland-Lang, A. D. Martin, P. Motylinski, and R. S. Thorne, Parton distributions in the LHC era: MMHT 2014 PDFs, Eur. Phys. J. C **75,** 204 (2015).

[81] J. Alwall, R. Frederix, S. Frixione, V. Hirschi, F. Maltoni, O. Mattelaer, H. S. Shao, T. Stelzer, P. Torrielli, and M. Zaro, The automated computation of tree-level and next-to-leading order differential cross sections, and their matching to parton shower simulations, J. High Energy Phys. 07 (2014) 079.

[82] Sensitivity projections for a search for new phenomena at high dilepton mass for the LHC Run 3 and the HL-LHC (2022).

[83] S. Schael *et al.* (ALEPH, DELPHI, L3, OPAL, LEP Electroweak Collaborations), Electroweak measurements in electron-positron collisions at W-boson-pair energies at LEP, Phys. Rep. **532,** 119 (2013).

[84] A. Angelescu, D. A. Faroughy, and O. Sumensari, Lepton flavor violation and dilepton tails at the LHC, Eur. Phys. J. C **80,** 641 (2020).

[85] M. S. Safronova, D. Budker, D. DeMille, D. F. J. Kimball, A. Derevianko, and C. W. Clark, Search for new physics with atoms and molecules, Rev. Mod. Phys. **90,** 025008 (2018).

[86] C. S. Wood, S. C. Bennett, D. Cho, B. P. Masterson, J. L. Roberts, C. E. Tanner, and C. E. Wieman, Measurement of parity nonconservation and an anapole moment in cesium, Science **275,** 1759 (1997).

[87] B. K. Sahoo, B. P. Das, and H. Spiesberger, New physics constraints from atomic parity violation in ^{133}Cs, Phys. Rev. D **103,** L111303 (2021).

[88] D. Becker *et al.*, The P2 experiment, Eur. Phys. J. A **54,** 208 (2018).

[89] P. S. B. Dev, W. Rodejohann, X.-J. Xu, and Y. Zhang, Searching for Z' bosons at the P2 experiment, J. High Energy Phys. 06 (2021) 039.

[90] I. Bischer, P. S. B. Dev, W. Rodejohann, X.-J. Xu, and Y. Zhang, Searching for new physics from SMEFT and leptoquarks at the P2 experiment, Phys. Rev. D **105,** 095016 (2022).

[91] R. Bause, H. Gisbert, M. Golz, and G. Hiller, Interplay of dineutrino modes with semileptonic rare B-decays, J. High Energy Phys. 12 (2021) 061.

[92] W. Altmannshofer and F. Archilli, Rare decays of b and c hadrons, in 2022 Snowmass Summer Study (2022), arXiv: 2206.11331.

[93] J. Aebischer, A. Crivellin, M. Fael, and C. Greub, Matching of gauge invariant dimension-six operators for $b \to s$ and $b \to c$ transitions, J. High Energy Phys. 05 (2016) 037.

[94] A. Celis, J. Fuentes-Martin, A. Vicente, and J. Virto, Gauge-invariant implications of the LHCb measurements on lepton-flavor nonuniversality, Phys. Rev. D **96,** 035026 (2017).

[95] J. E. Camargo-Molina, A. Celis, and D. A. Faroughy, Anomalies in bottom from new physics in top, Phys. Lett. B **784,** 284 (2018).

[96] S. Bißmann, J. Erdmann, C. Grunwald, G. Hiller, and K. Kröninger, Constraining top-quark couplings combining top-quark and **B** decay observables, Eur. Phys. J. C **80,** 136 (2020).

[97] R. Aoude, T. Hurth, S. Renner, and W. Shepherd, The impact of flavour data on global fits of the MFV SMEFT, J. High Energy Phys. 12 (2020) 113.

[98] S. Bißmann, C. Grunwald, G. Hiller, and K. Kröninger, Top and beauty synergies in SMEFT-fits at present and future colliders, J. High Energy Phys. 06 (2021) 010.

[99] S. Bruggisser, R. Schäfer, D. van Dyk, and S. Westhoff, The flavor of UV physics, J. High Energy Phys. 05 (2021) 257.

[100] W. Altmannshofer and P. Stangl, New physics in rare B decays after Moriond 2021, Eur. Phys. J. C **81,** 952 (2021).

[101] R. Aaij *et al.* (LHCb Collaboration), Test of lepton universality with $B^0 \to K^{*0}\ell^+\ell^-$ decays, J. High Energy Phys. 08 (2017) 055.

[102] R. Aaij *et al.* (LHCb Collaboration), Test of lepton universality with $\Lambda_b^0 \to pK^-\ell^+\ell^-$ decays, J. High Energy Phys. 05 (2020) 040.

[103] R. Aaij *et al.* (LHCb Collaboration), Tests of Lepton Universality Using $B^0 \to K_S^0\ell^+\ell^-$ and $B^+ \to K^{*+}\ell^+\ell^-$ Decays, Phys. Rev. Lett. **128,** 191802 (2022).

[104] R. Aaij *et al.* (LHCb Collaboration), Test of lepton universality in beauty-quark decays, Nat. Phys. **18,** 277 (2022).

[105] R. Aaij *et al.* (LHCb Collaboration), Measurement of CP-Averaged Observables in the $B^0 \to K^{*0}\mu^+\mu^-$ Decay, Phys. Rev. Lett. **125,** 011802 (2020).

[106] R. Aaij *et al.* (LHCb Collaboration), Differential branching fractions and isospin asymmetries of $B \to K^{(*)}\mu^+\mu^-$ decays, J. High Energy Phys. 06 (2014) 133.

[107] R. Aaij *et al.* (LHCb Collaboration), Measurements of the S-wave fraction in $B^0 \to K^+\pi^-\mu^+\mu^-$ decays and the $B^0 \to K^*(892)^0\mu^+\mu^-$ differential branching fraction, J. High Energy Phys. 11 (2016) 047; 04 (2017) 142(E).

[108] R. Aaij *et al.* (LHCb Collaboration), Branching Fraction Measurements of the Rare $B_s^0 \to \phi\mu^+\mu^-$ and $B_s^0 \to f_2'(1525)\mu^+\mu^-$ Decays, Phys. Rev. Lett. **127,** 151801 (2021).

[109] D. Bečirević and O. Sumensari, A leptoquark model to accommodate $R_K^{\mathrm{exp}} < R_K^{\mathrm{SM}}$ and $R_{K^*}^{\mathrm{exp}} < R_{K^*}^{\mathrm{SM}}$, J. High Energy Phys. 08 (2017) 104.

[110] J. F. Kamenik, Y. Soreq, and J. Zupan, Lepton flavor universality violation without new sources of quark flavor violation, Phys. Rev. D **97,** 035002 (2018).

[111] P. J. Fox, I. Low, and Y. Zhang, Top-philic Z' forces at the LHC, J. High Energy Phys. 03 (2018) 074.

[112] R. Coy, M. Frigerio, F. Mescia, and O. Sumensari, New physics in $b \to s\ell\ell$ transitions at one loop, Eur. Phys. J. C **80,** 52 (2020).

[113] X.-Q. Li, M. Shen, D.-Y. Wang, Y.-D. Yang, and X.-B. Yuan, Explaining the $b \to s\ell^+\ell^-$ anomalies in Z' scenarios with top-FCNC couplings, Nucl. Phys. **B980,** 115828 (2022).

[114] LHCb Collaboration, Test of lepton universality in $b \to s\ell^+\ell^-$ decays, arXiv:2212.09152.

[115] LHCb Collaboration, Measurement of lepton universality parameters in $B^+ \to K^+\ell^+\ell^-$ and $B^0 \to K^{*0}\ell^+\ell^-$ decays, arXiv:2212.09153.

[116] CMS Collaboration, Measurement of $B_s^0 \to \mu^+\mu^-$ decay properties and search for the $B^0 \to \mu\mu$ decay in proton-proton collisions at $\sqrt{s} = 13$ TeV, arXiv:2212.10311.

[117] M. Ciuchini, M. Fedele, E. Franco, A. Paul, L. Silvestrini, and M. Valli, Constraints on lepton universality violation from rare B decays, Phys. Rev. D **107,** 055036 (2023).

[118] Y. Amhis *et al.* (HFLAV Collaboration), Averages of b-hadron, c-hadron, and τ-lepton properties as of 2021, Phys. Rev. D **107,** 052008 (2023).

[119] S. Wehle *et al.* (Belle Collaboration), Lepton-Flavor-Dependent Angular Analysis of $B \to K^*\ell^+\ell^-$, Phys. Rev. Lett. **118,** 111801 (2017).

[120] S. Choudhury *et al.* (BELLE Collaboration), Test of lepton flavor universality and search for lepton flavor violation in $B \to K\ell\ell$ decays, J. High Energy Phys. 03 (2021) 105.

[121] A. Abdesselam *et al.* (Belle Collaboration), Test of Lepton-Flavor Universality in $B \to K^*\ell^+\ell^-$ Decays at Belle, Phys. Rev. Lett. **126,** 161801 (2021).

[122] D. M. Straub, flavio: A Python package for flavour and precision phenomenology in the Standard Model and beyond, arXiv:1810.08132.

[123] R. L. Workman *et al.* (Particle Data Group), Review of particle physics, Prog. Theor. Exp. Phys. **2022,** 083C01 (2022).

[124] S. Davidson and A. Saporta, Constraints on $2\ell 2q$ operators from $\mu - e$ flavour-changing meson decays, Phys. Rev. D **99,** 015032 (2019).

[125] M. Carpentier and S. Davidson, Constraints on two-lepton, two quark operators, Eur. Phys. J. C **70,** 1071 (2010).

[126] S. Schael *et al.* (ALEPH, DELPHI, L3, OPAL, SLD, LEP Electroweak Working Group, SLD Electroweak Group, SLD Heavy Flavour Group Collaborations), Precision electroweak measurements on the Z resonance, Phys. Rep. **427,** 257 (2006).

[127] J. Benesch *et al.* (MOLLER Collaboration), The MOLLER experiment: An ultra-precise measurement of the weak mixing angle using Møller scattering, arXiv:1411.4088.

[128] Y. Du, A. Freitas, H. H. Patel, and M. J. Ramsey-Musolf, Parity-Violating Møller Scattering at Next-to-Next-to-Leading Order: Closed Fermion Loops, Phys. Rev. Lett. **126,** 131801 (2021).

[129] E. E. Jenkins, A. V. Manohar, and M. Trott, Renormalization group evolution of the standard model dimension six operators II: Yukawa dependence, J. High Energy Phys. 01 (2014) 035.

[130] R. Alonso, E. E. Jenkins, A. V. Manohar, and M. Trott, Renormalization group evolution of the standard model dimension six operators III: Gauge coupling dependence and phenomenology, J. High Energy Phys. 04 (2014) 159.

[131] E. E. Jenkins, A. V. Manohar, and P. Stoffer, Low-energy effective field theory below the electroweak scale: Operators and matching, J. High Energy Phys. 03 (2021) 016.

[132] E. E. Jenkins, A. V. Manohar, and P. Stoffer, Low-energy effective field theory below the electroweak scale: Anomalous dimensions, J. High Energy Phys. 01 (2021) 084.

[133] A. Czarnecki and W. J. Marciano, Electroweak radiative corrections to polarized Moller scattering asymmetries, Phys. Rev. D **53,** 1066 (1996).

[134] FQXi.org.